

**INVESTIGATIONS INTO THE SYNTHESIS, IDENTIFICATION, AND
DEVELOPABILITY OF ACTIVE IONIC LIQUIDS**

**BY
ELISE MILLER**

Submitted to the graduate degree program in Pharmaceutical Chemistry and the Graduate
Faculty of the University of Kansas in partial fulfilment of the requirements for the
degree of Master of Arts

John Stobaugh

Laird Forrest

W. Peter Wuelfing

Date Defended: November 28, 2012

The Thesis Committee for Elise Miller
certifies that this is the approved version of the following thesis:

Investigations into the Synthesis, Identification,
and Developability of Active Ionic Liquids

Chairperson: John Stobaugh

Date approved: November 28, 2012

Abstract

Studied for decades, ionic liquids have largely been used as solvents in the pharmaceutical industry. An active ionic liquid (AIL) contains an active pharmaceutical ingredient (API) as one of the counterions. They have the potential to be advantageous in traditional oral and alternative non-oral routes of administration. The library of successful AILs was increased with a series of generic and proprietary compounds. They were characterized via infrared spectrometry, glass transition temperature, residual solvent, salt factor and biorelevant solubility. The impact of counterion selection on physical properties was discussed for three series of AILs. Issues with purification and the impact of residual solvent were investigated. While the equilibrium solubility enhancement of AILs over their neutral forms was not as high as hoped for, the dissolution rate advantage and utility for liquid dosing remains to be investigated.

Acknowledgements

W. Peter Wuelfing – onsite advisor

John Stobaugh – faculty advisor

John Higgins

Allen Templeton

Mike Kress

Monica Tijerina

Sophie-Dorothee Clas

Justin Belardi

Chuck Pratt

Scott Ceglia

Laird Forrest

Table of Contents

Section	Page
Title Page	i
Acceptance Page	ii
Abstract	iii
Acknowledgements	iv
List of Tables	vi
List of Figures	vii
List of Equations	viii
List of Abbreviations	ix
Introduction	1
Experimental	6
Results	15
Discussion	31
Conclusion	41
References	42
Appendices	44

List of Tables

Table Number	Page
Table 1. Medium Throughput Screen with Results: L = Liquid and S = Solid	20
Table 2. Percent weight loss by 100°C (RS), Glass Transition Temperature (Tg) and Melting Points (Tm) of Attempted Active Ionic Liquids	22
Table 3. Viscosity at various temperatures for four Active Ionic Liquids	24
Table 4. Identifying Peaks for Salt Formation of Lidocaine Ionic Liquids	25
Table 5. ^1H NMR Spectra for Lidocaine Salicylate and Propantheline Tosylate	26
Table 6. Salt Factor of ionic liquids and Solubility of ionic liquids compared to free form at 2 and 24 hours.	30

List of Figures

Figure Number	Page
Figure 1. Active compounds and counterions. * Acids used in medium throughput screen. ★ Negative control active acidic compounds not expected to form an ionic bond with acidic counterions.	18
Figure 2. Lidocaine standard (red), Benzoic acid standard (black), and Lidocaine benzoate (blue) overlaid IR spectra.	25
Figure 3. Lidocaine with nicotinic acid sample (pink) and lidocaine standard (red) XRD patterns	27
Figure 4. Plot of the percent weight gain by lidocaine salicylate batch 3b sample vs. time (blue line) and the measured relative humidity of the sample chamber vs. time (green line).	29

List of Equations

Equation Number	Page
Equation 1. Gibbs Free Energy	1
Equation 2. Gibbs Free Energy rearranged for Melting Point Determination	1
Equation 3. Kapustinkii	2

List of Abbreviations

AIL – Active Ionic Liquid
API – Active Pharmaceutical Ingredient
ATR - Attenuated Total Reflectance mode of Infrared Spectroscopy
BA – Benzoic Acid
CA – Citric Acid
CI – Counterion
 $\Delta_{\text{fus}}G$ – Change in Gibbs Free Energy upon Fusion
 ΔH – Change in Enthalpy
 ΔS – Change in Entropy
DMSO – Dimethyl Sulfoxide
DSC - Differential Scanning Calorimetry
DVS – Dynamic Vapor Sorption
FaSSIF – Fasted State Simulated Intestinal Fluid
FTIR – Fourier Transform Infrared Spectroscopy
G - Gibbs Free Energy
GC - Gas Chromatography
HPLC - High Performance Liquid Chromatography
KF - Karl Fisher Titration
L – Liquid result in Medium Throughput Screen
MA – Malic Acid
MdA – Mandelic Acid
mDSC – Modulated Differential Scanning Calorimetry
MK-x – Proprietary Merck compound
NM – Not Measured
NMR – Nuclear Magnetic Resonance
RH – Relative Humidity
RS – Residual Solvent
RTIL – Room Temperature Ionic Liquid
S – Solid result in Medium Throughput Screen
SGF – Simulated Gastric Fluid
SIF – Simulated Intestinal Fluid
T - Temperature
T_g – Glass Transition Temperature
TGA - Thermogravimetric Analysis
T_m – Melting Point
TsA – *p*-Toluenesulfonic Acid
TW80 – Tween 80
XRD – X-ray Diffraction

Introduction

Salt forms of pharmaceuticals can have a large impact on solubility, stability, manufacturing properties and ultimately bioavailability¹. While resources can be devoted to finding the most stable polymorph of the chosen salt early in development, detrimental polymorphic changes can occur at any point in development and manufacture. Polymorph screens and extended stability testing cannot account for all changes and stressors that a drug will encounter². A low solubility phase can be developed by stabilizing the more soluble amorphous phase of the compound within a polymer matrix, called an amorphous solid dispersion. Major downsides to this method are the expensive manufacturing equipment needed, increased excipient loading in the product due to the polymer and the risk of crystallization from the meta-stable system³. The polymer matrix can temporarily stabilize the high energy amorphous phase, but many factors can induce nucleation and growth of crystal seeds like heat or moisture³. A relatively new approach to increase solubility is to make a salt that is molten at room temperature, called an ionic liquid^{1,2,4-6}.

Technically, ionic liquids are salts that have a melting point below 100°C. Of greater interest are room temperature ionic liquids (RTIL)^{1,2,4-6}. As the name suggests, ionic liquids are defined by both their physical liquid state and a full ionic bond between the components.⁷ An investigation into the properties of ionic liquids shows an interesting relationship between entropy and enthalpy in determining the Gibbs free energy of fusion for the system, equation 1.⁸

$$\Delta_{\text{fus}}G = \Delta H - T\Delta S \quad (1)$$

$$T_m = \Delta H_m / \Delta S_m \quad (2)$$

The solid will undergo fusion (melt to form a liquid) when the $\Delta_{\text{fus}}G = 0$. When $\Delta_{\text{fus}}G < 0$, the liquid state is favored⁹. According to equation 2, the ratio of ΔH_m over ΔS_m must equal a temperature below 100°C for an IL or below ambient temperature for a RTIL. Since the formation of a crystalline lattice would increase the order in the system and thus decrease the entropy, the role of entropy in eqs 1 & 2 is already in favor of a liquid. The stability increase in a crystalline phase comes primarily from the enthalpy term in the eq. 1. Enthalpy in the system can be controlled through decreasing the lattice energy by increasing the radii of the ions based on the Kapustinkii equation (equation 3) where U_L = Lattice energy, K and d are constants, v = number of ions in empirical formula, z = numbers of elementary charges on ions, r = radii of ions¹⁰.

$$U_L = -K \cdot \frac{v \cdot |z^+| \cdot |z^-|}{r^+ + r^-} \cdot \left(1 - \frac{d}{r^+ + r^-}\right) \quad (3)$$

Decreasing symmetry in the ionic structure can also decrease crystallization tendency. Another approach to decrease crystallization tendency utilizes the importance of hydrogen bonding to create the crystal lattice. The phrase "anti-crystal engineering" was coined to describe actively picking cations and anions that will not form hydrogen bond donor and acceptor pairs and thus are more likely to form a stable IL¹.

Studied for decades, ionic liquids have largely been used as solvents in the pharmaceutical industry. An active ionic liquid (AIL) contains an active pharmaceutical ingredient (API) as one of the counterions. They are potentially advantageous in traditional oral and alternative non-oral routes of administration. Just as the solubility of a crystalline salt can be modulated with the creative use of counter-ions, AILs have the potential of higher solubility than the parent

compound. By presenting the compound in a molten state in an oral formulation, problems of dissolution-rate limited absorption may be avoided, as with a liquid filled capsule. Their liquidity is well-suited for transdermal, intraoral, ocular, and intranasal administration. The current intellectual property environment has lead to increased importance of alternative administration routes as a means of extending exclusivity potentially past patent expiration¹¹.

There are risks involved in developing an AIL. Like amorphous compounds, the threat of crystallization should be evaluated through extensive phase and formulation stability testing². The liquid phase is stable; however, crystalline solvates or cocrystals may form over time. Purity is also a concern with ionic liquids¹². Solvent from the salt formation and absorbed atmospheric moisture are the most challenging to remove. Typically the crystallization step is used as a final purification step, removing impurities from the lattice¹². Solid impurities are not removed in the creation of a crystal lattice for AILs. Crystalline salts are typically made with a slight excess of counterion to insure the reaction proceeds to completion. A metathesis reaction, or double replacement reaction between two existing salts that exchange equimolar amount of counterion, to form an IL and an insoluble salt would allow the excess to be filtered from the IL product or isolated in a non-miscible organic phase along with the insoluble by-product¹². Impurities can inhibit crystallization, thus artificially forming an ionic liquid¹⁰. Due to the plasticizing effect of water and other solvents, all characterization data should be supplied with a reference to the dryness of the sample¹⁰. Viscosity can also be an issue with AILs that the proper choice of counter-ion can negate². Not discussed in the literature, the difficulty of handling high viscosity liquids would need to be addressed before an AIL is chosen as a final phase. Equipment designed

to operate at elevated temperature with proper controls around water and temperature variation may be needed.

The study of active ionic liquids to date mainly involves synthesis and limited physical characterization. Solubility claims have not been supported by empirical data.^{1,2,4,5,13}. Furthermore, AILs have yet to be proven practically useful in industrial pharmaceutical development. Missing are comparisons of the AIL and crystalline salt forms by solubility in biorelevant media, solubility/miscibility in dosing vehicles, and bioavailability in preclinical species. Without head to head comparison, the advantages of AILs for drug delivery are all hypothetical. Very few actual pharmaceutical actives and counterions have been reported to make AILs¹⁴. The research herein aims to provide data to work towards an answer to the developability of active ionic liquids.

For this research, two model AILs from the literature were made to gain an understanding of the synthesis and characterization of liquid actives before novel AILs were attempted. Propantheline tosylate and Lidocaine salicylate were chosen because of the availability of starting material and differing isolation procedures^{1,6}. Then, the solubility in biorelevant GI media was compared to the parent forms, Propantheline Bromide and Lidocaine free base. Novel ionic liquids were attempted, first with lidocaine and then with other generic and Merck compounds. The current pool of counter-ions for IL formation consists of the sixty or so commonly used pharmaceutical salts and essentially all GRAS compounds capable of forming an ionic liquid with an API¹⁵. High throughput screening is necessary for active ionic liquids to become an available tool in salt selection for industrial pharma¹⁶. It was hypothesized that one could directly use or slightly

modify existing high throughput salt screens for AIL screening. The experimental methodology of an automated system in a 96-well plate was directly transferred to a medium through-put design. The "medium" descriptor indicates that all samples were manually aliquoted instead of using a robotic liquid handler. The screen was successfully developed on a 96-well plate and in total seven generic compounds and 11 Merck compounds were screened with benzoic acid, malic acid, mandelic acid, citric acid, and p-toluenesulfonic acid. Only this small subset of pharmaceutically acceptable acids was used in the screen, chosen by the following rationale. Toluenesulfonic acid was included because of past precedence in making an ionic liquid with propantheline. Citric acid is a common pharmaceutically acceptable counterion with a large ionic radius, which should decrease the likelihood of crystallization according to Kapustinkii equation. However it does have multiple hydrogen bond donors and acceptors in a symmetrical arrangement to stabilize a crystalline phase. Benzoic, mandelic, and malic acids are structurally similar to salicylic acid, which is known to make an ionic liquid with lidocaine. They are all large ions compared to the most common pharmaceutical ions of chlorine and sodium¹⁷. Screening a series of phenyl carboxylic acid allows structure – property relationships to be investigated based on which ionic liquids are formed.

Experimental

Chemicals used in the synthesis and characterization of AILs

1.0 N hydrochloric acid, citric acid, glacial acetic acid, succinic acid, acetonitrile, acetone, dichloromethane, and 85% phosphoric acid in water were purchased from Fisher Scientific. Tween 80, methanesulfonic acid, mandelic acid, malic acid, and fumaric acid were purchased from Acros Organics. Lidocaine and itraconazole were purchased from Spectrum. Propantheline bromide was purchased from MP Biomedicals, LLC. SIF powder for biorelevant solubility was purchased from Phares. Ketoconazole was purchased from TCI. Piroxicam, lysine, acetaminophen, tolfenamic acid, indomethacin, ketoprofen, *p*-toluenesulfonic acid, salicylic acid, nicotinic acid, glutamic acid, benzoic acid, and silver toluenesulfonate were purchased from Sigma Aldrich. All Merck proprietary compounds (MK-x) were synthesized by Merck Research Laboratories, Rahway, New Jersey.

Analysis

Differential Scanning Calorimetry

Differential Scanning Calorimetry (DSC) experiments were run on a TA Instruments, New Castle, Delaware, Differential Scanning Calorimeter model Q2000-1086 in standard mode in a crimped aluminum pan, with an empty crimped aluminum pan as the reference. Experimental condition: Equilibrate at 25°C then ramp 10°C / min to 300°C. Data sampling occurred every 0.20 sec/point.

Modulated Differential Scanning Calorimetry

Modulated Differential Scanning Calorimetry (mDSC) experiments were run on a TA Instruments, New Castle, Delaware, Differential Scanning Calorimeter model Q2000-1086 in modulated mode in a crimped aluminum pan, with an empty crimped aluminum pan as the reference. Experimental condition: Equilibrate at -20°C; isothermal hold for 2 min.; modulate +/- 0.5°C every 60 sec; ramp 2°C /min to 100°C; mark end of cycle 1; ramp 5°C /min to -20°C; repeat isothermal hold and modulated ramp for two more cycles, with data sampling at 0.20 sec/point. Cycle 1 data was reported.

Thermogravimetric Analysis

Thermogravimetric Analysis (TGA) analysis was performed on a TA Instruments, New Castle, Delaware, Thermogravimetric Analysis Infrared model Q5000-0288 using a ramp method, heating at 10.0°C /min from room temperature to 300°C or 500°C. Data was collected every 0.5 sec, after the weight had stabilized.

Dynamic Vapor Sorption

Dynamic Vapor Sorption (DVS) analysis was run on a TA Instruments, New Castle, Delaware, Thermogravimetric Analysis Sorption Analysis model Q-5000-5059. The sample was dried at 60°C until stabilized to 0.1% by weight for 5 min or a maximum dwell time of 60 min. The experiment for lidocaine salicylate and lidocaine benzoate were run at 25°C with an initial relative humidity (RH) of 5%, ramping to 95% RH and back to 5% RH in 5% increments after the sample stabilized to 0.1% for 5 min or a max dwell time of 180 min. The experiment for Propantheline tosylate was run at 40°C with an initial RH of 5%, ramping to 95% RH and back

to 5% RH in 5% increments after the sample stabilized to 0.1% for 5 min or a max dwell time of 360 min. Data for both samples was collected every 5 sec.

Equilibrium Solubility and Salt Factor

Vehicle Preparation: Standard Gastric Fluid (SGF) was prepared by adding 2.0 g of sodium chloride and 16.8 mL of 1.0N HCl to a 1L bottle and diluting to 1.0 L with deionized water. Fasted State Simulated Intestinal Fluid (FaSSIF) was prepared by diluting 2.24 g of Phares Standard Intestinal Fluid (SIF) powder to 1.0 L of 30 mM phosphate buffer, pH 6.5. The buffer was prepared by adding 3.44 g of sodium dihydrogen phosphate, 0.420 g of solid sodium hydroxide, and 6.20 g of sodium chloride to a 1 L bottle. The solids were dissolved with 1.0 L of deionized water. The 10% Tween 80 (TW80) vehicle was prepared by diluting 100 mL of TW80 to 1.0 L with deionized water.

Equilibrium solubility sample preparation: samples were heated on a 60°C hot plate for 10 min to increase flow, and then approximately 5 mg of salt was transferred to tared 1.5 mL centrifuge tubes to which 100 µL of vehicle was added. The samples were mixed on a stir plate at 400 rpm, ambient temperature for 24 hours, with an interim measurement at 2 hours. At 2 hours and at 24 hours, the samples were centrifuged at 21,100 xg using a Thermo Scientific, Waltham, Massachusetts, model Sorvall Legend Micro 21R centrifuge for 20 minutes. To a 1.5 mL vial, 10 µL of supernatant was transferred and 1000 µL of acetonitrile: water (1:1) diluent was added. The sample was mixed by inversion before injection. All solubility samples had a 101 dilution factor. For preparation of salt and active parent standards for weight based assay to determine the salt factor, approximately 2.5 mg of parent or salt was weighed into a tared 25 mL volumetric

flask, then filled to volume with diluent of acetonitrile: water (1:1) and mixed on a stir plate overnight.

High Performance Liquid Chromatography

High Performance Liquid Chromatography (HPLC) analysis was performed using an Agilent, Santa Clara, California, model 1100 system. A 6 min gradient was used to resolve sample at 40°C ramping from 10% acetonitrile, 90% (0.1% Phosphoric acid in water) to 90% acetonitrile in 5 min. The gradient was then decreased to 10% acetonitrile and held for 1 min. An Ascentis Fused Core, 4.6 x 100 mm, 2.7 μm particle size, C18 column was used.

Rheometry

Viscosity was measured with a TA Instruments, New Castle, Delaware, Rheometer model AR15000 with Rheology Advantage Control AR software and a 20 mm aluminum plate. All samples were tested under a 500 μm gap with the plate rotating from 0 $\pi^*\text{rad/sec}$ to 500 $\pi^*\text{rad/sec}$ over 10 min.

Fourier Transform Infrared Spectroscopy

Attenuated Total Reflectance mode Fourier Transform Infrared Absorption (ATR FTIR) analysis was conducted with a Perkin Elmer, Waltham, Massachusetts, model Spectrum 100 FT-IR spectrometer. The analysis was performed between 515 cm^{-1} and 4000 cm^{-1} with three runs averaged to produce a spectrum.

X-Ray Diffraction

X-Ray Diffraction (XRD) was performed using a Rigaku, The Woodlands, Texas, model Miniflex II XRD operating in reflectance mode, with data sampling every 0.02 °2θ with 1.0 sec per °2θ from 2.5° 2θ to 40° 2θ. Fixed mode operation at 30 kv and 15 mA. Integrated X-Ray Powder Diffraction Software, PDXL Qualitative analysis was used.

Proton Nuclear Magnetic Resonance Spectrometry

Proton Nuclear Magnetic Resonance (^1H NMR) spectra were collected on active ionic liquid samples and the active parent and counterions as reference using a Varian, Palo Alto, model Inova 400 MHz spectrometer using d^6 -dimethyl sulfoxide (DMSO) as solvent.

Synthesis

Propantehline Tosylate: Silver Halide Precipitation Method

Propantehline tosylate was prepared on a 2.5 g scale via a methathesis reaction of Propantheline Bromide and silver *p*-toluenesulfonate¹. Starting material was mixed in 100 mL of methanol overnight, protected from light. The solids were filtered through 0.22 μm Millex Durapore PVDF syringe filters. The majority of the solvent was removed via rotary evaporation, with the remaining solvent removed under high vacuum for 2 hours. The sample had solid amorphous and crystalline particles visible by polarized light microscopy. The sample was taken up in 10 mL of methanol and re-filtered through a new 0.22 μm filter again into a round bottom flask. The flask was attached to a Büchi, Flawil, Switzerland, model Rotavapor R200 with the bottom of the flask immersed in a Büchi, Flawil, Switzerland, model B490 heating bath set to 40°C. The majority of the solvent was removed under a vacuum controlled by a KNF, Freiburg, Germany, model Neuberger Vacuum pump controller set to 20mBar. The vacuum was achieved using a KNF,

Freiburg, Germany, model Laboport Pump. The remaining solvent removed under 2mBar pressure vacuum for 2 hours. The sample was analyzed by mDSC, TGA, NMR, FTIR, rheometry, and DVS. Equilibrium solubility of the AIL and the active parent were measured.

Lidocaine Salicylate: Hot Melt Method

Lidocaine Salicylate was prepared on a 800 mg (Batch 1), then an 8 g (Batch 2) scale by adding equimolar amounts of Lidocaine and salicylic acid in 20mL scintillation vials, stirring the dry powder with a spatula to homogenize the mixture, and then heating to 100°C on a heated stir plate. In both batches, the mixture melted within 10min of heating to form a clear, viscous solution. Upon cooling, the liquid increased in viscosity until effectively solid. The samples were heated to 100°C on a hot plate to allow easier aliquots to be taken for modulated DSC and TGA (batch 2 only).

Lidocaine Salicylate: Organic Extraction Method

Lidocaine Salicylate was prepared on a 15 g scale (Batch 3), by adding molar equivalents of Lidocaine and salicylic acid to a 250 mL round bottom flask and dissolving the compounds in 100mL of 1:1 acetone: water. The solution was stirred overnight using a IKA, Wilmington, North Carolina, RCT Basic stir plate with reaction vessel attachment at room temperature⁶. The sample was diluted with 100 mL of water then extracted with several washings of dichloromethane. The isolated organic layer was dried with about 5g of sodium sulfate transferred to a new round bottom flask. The flask was attached to a Büchi, Flawil, Switzerland, model Rotavapor R200 with the bottom of the flask immersed in a Büchi, Flawil, Switzerland, model B490 heating bath set to 40°C. The majority of the solvent was removed under a vacuum

controlled by a KNF, Freiburg, Germany, model Neuberger Vacuum pump controller set to 20 mBar. The vacuum was achieved using a KNF, Freiburg, Germany, model Laboport Pump. Analysis was performed using mDSC, TGA, and DVS, FTIR and rheometry. H^1 NMR spectra of starting material and sample collected. The sample was sent to an analytical department to test for residual solvent by Gas Chromatography (GC) and Karl Fisher Titration (KF). Based on GC and KF results, the sample was further dried under 2 mBar vacuum (Batch 3b). The glass transition temperature and residual solvent were remeasured. Equilibrium solubility of the AIL and the active parent were measured.

Lidocaine based Ionic Liquids: Hot Melt Method

Lidocainium benzoate, mandelate, malate, tosylate, nicotinate, and fumarate salts were prepared at an 800 mg scale by adding equimolar amounts of Lidocaine and counterion in the acidic form to 4 mL scintillation vials or 25 mL round bottomed flasks. The dry powder was stirred initially with a spatula to homogenize mixture. The mixtures were heated to 60°C on using an IKA, Wilmington, North Carolina, RCT Basic stir plate with reaction vessel attachment while stirring with a magnetic stir bar. In the benzoate, mandelate, and malate samples, the mixture melted within 10min of heating to form a clear, viscous liquid. The nicotinate, fumarate, and toluenesulfonate samples did not form liquids. The liquid samples were analyzed using mDSC, TGA, FT-IR and rheometry. The solid samples were analyzed using DSC, TGA, FTIR, and XRD. Equilibrium solubility of the AIL and the active parent were measured.

Piroxicam, Tolfenamic Acid and Merck A: Organic Extraction Method

Samples were prepared on a 1 g scale by adding molar equivalents of both counterions in a 250mL round bottom flask, and dissolving in 100 mL of solvent and stirring overnight at room temperature. The HCl salt of MK-A was reacted with glutamic acid, methanesulfonic acid, succinic acid, and sodium acetate, dissolved in acetonitrile. The neutral form of piroxicam was reacted with p-toluenesulfonic acid and citric acid as a solution in dichloromethane. Tolfenamic acid was reacted with L-lysine and lidocaine as a solution in 1:1 acetonitrile: water. The samples were diluted with 100 mL of water then extracted with several washings of dichloromethane. The isolated organic layer was dried with about 5 g of sodium sulfate then filtered through celite into a round bottom flask. The flask was attached to a Büchi, Flawil, Switzerland, model Rotavapor R200 with the bottom of the flask immersed in a Büchi, Flawil, Switzerland, model B490 heating bath set to 40°C. The majority of the solvent was removed under a vacuum controlled by a KNF, Freiburg, Germany, model Neuberger Vacuum pump controller set to 20 mBar. The vacuum was achieved using a KNF, Freiburg, Germany, model Laboport Pump. The solid samples were analyzed using DSC, TGA, and XRD. Spectra and graphs are located in the appendices.

Medium Throughput Screen and Scale-up

The basic compounds included in the screen were itraconazole, ketoconazole, and MK- B, C, D, E, G, H, J, K, and M. Three acidic generic compounds, acetaminophen, indomethacin, and ketoprofen, and two Merck acidic compounds, MK-F and MK-L, were included as negative controls. The counterions are benzoic acid, mandelic acid, malic acid, p-toluenesulfonic acid, and citric acid. Stock solutions of all active compounds and counterions were prepared at 0.1 M concentration in various solvents to allow for ease of transfer to well plates. All were prepared at

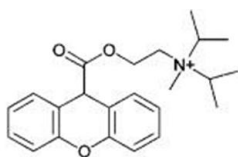
a 1:1 molar equivalent of active and counterion with 100 μ L of each being added to a well. The actives are listed in Table 1 along with the solvents used and screening hits. The plates were mixed on a shaker/mixer for 30 min, and then the solvent was evaporated in a fume hood overnight. A hit was defined as a sample having no visible solids after evaporation. They are labeled "L" in Table 1, while samples with visible solids are labeled "S". Hits for MK-C, MK-D, MK-B, acetaminophen, and itraconazole were repeated at a larger scale. Due to limited compound availability and numerous hits, MK-C was only scaled up to 50 mg active samples. The others were scaled up to 0.5 g – 1.0 g active samples. These batches were prepared identically to the screening samples. Compound and acid were added in equimolar amounts to either 4 or 20 mL scintillation vials, dissolved with solvent and heated to 60°C using an IKA, Wilmington, North Carolina, RCT Basic stir plate with reaction vessel attachment to allow for evaporation of solvent. DSC was performed on samples with visible solids while mDSC and TGA were performed on the potential ionic liquids. The results from the scale up are in Table 2. Samples with solids have an indicated melting point and samples that were potential ionic liquids have a glass transition temperature (T_g) listed. Equilibrium solubility of the AIL and the active parent, except for ketoprofen, were measured.

Results

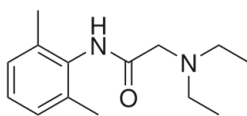
Medium Throughput Screen

The AILs medium throughput screen was implemented for a total of 16 generic and Merck compounds. Acetaminophen, indomethacin, ketoprofen, MK-F and MK-L are acidic compounds, which were included in the screen as negative controls. Active compound and counterion structures of all samples are depicted in Figure 1. Since there are numerous scenarios that produce a liquid, such as impurities, excess solvent, hydrogen bonding, and mixtures of ionic and hydrogen bonding, the ability of the screen to produce all these products needs to be known¹⁸. Precipitated solids, labeled “S” in Table 1, were obvious by observing small particles or crystals growing in the wells. Samples that were deemed hits were scaled up and labeled “L” in the table. Abbreviations for the counterions used in Table 1 are as follows: counterions (CI), benzoic acid (BA), malic acid (MA), *p*-toluenesulfonic acid (TsA), mandelic acid (MdA), and citric acid (CA). The 1 g samples of Merck K tosylate, Merck J tosylate, all Merck H salt hits, and ketoconazole benzoate produced solids and no further characterization was conducted.

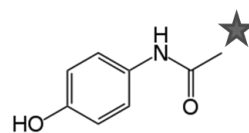
Active Compounds



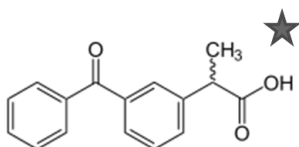
Propantheline



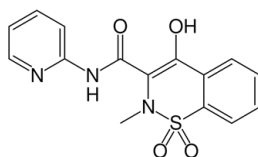
Lidocaine



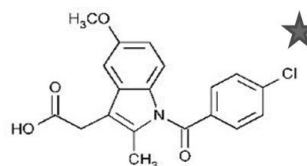
Acetaminophen



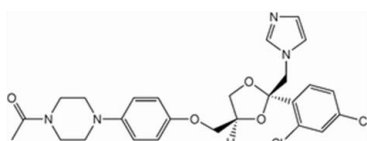
Ketoprofen



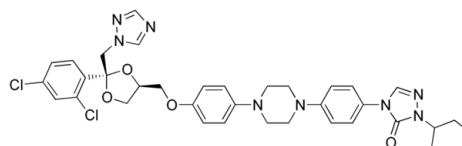
Piroxicam



Indomethacin

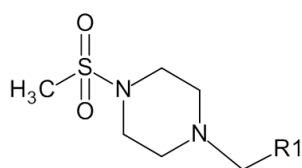


Ketoconazole

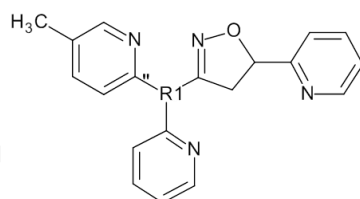


Itraconazole

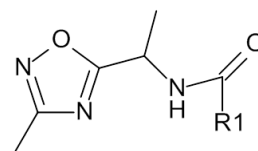
Merck Proprietary Active Compounds



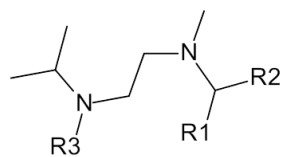
MK-A



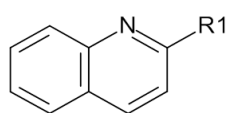
MK-B



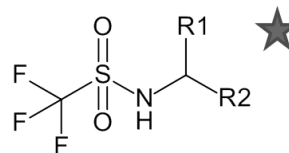
MK-C



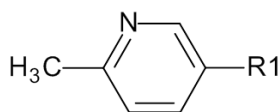
MK-D



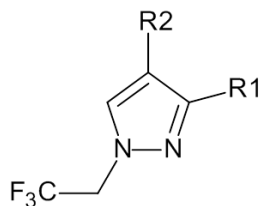
MK-E



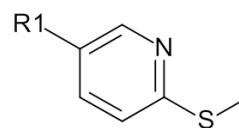
MK-F



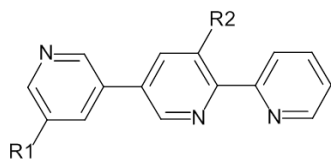
MK-G



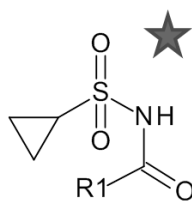
MK-H



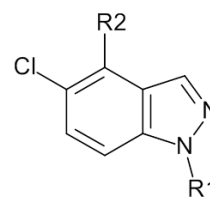
MK-J



MK-K

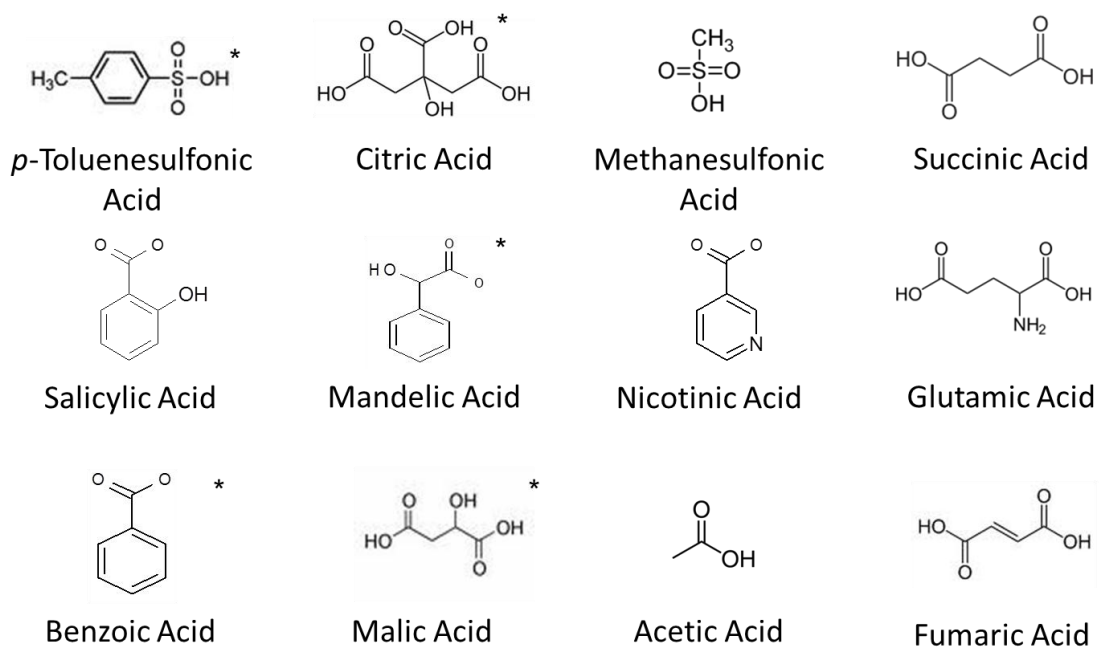


MK-L



MK-M

Acidic Counterions



Acidic Active and Basic Counterion

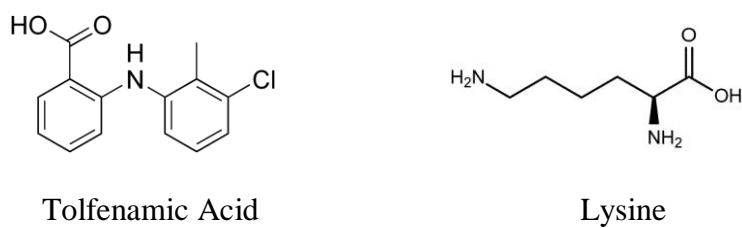


Figure 1. Active compounds and counterions. * Acids used in medium throughput screen.

★ Negative control active acidic compounds not expected to form an ionic bond with acidic counterions.

Indomethacin, MK-F and MK-L, all acidic parent compounds, did not produce hits in the screen. Acetaminophen tosylate and ketoprofen malate, mandelate, and tosylate did result in screen hits. When reacted at a 1g scale, the acetaminophen tosylate formed a crystalline solid. The ketoprofen salts formed meta-stable liquids that all eventually crystallized after several weeks of ambient storage. This was predicted in the tosylate salt from the melting endotherm present at 77°C. The 1.0 g scale of MK-A salts were all crystalline with the melting point listed in Table 2.

Table 1. Medium Throughput Screen with Results: L = Liquid and S = Solid

	CI	BA	MA	TsA	MdA	CA
Parent Compound	pKa	4.2	3.5, 5.1	-1.34	3.37	3.1, 4.8
MK-B	4, 4.5, 13	S	S	L	S	S
MK-F	5.37	S	S	S	S	S
MK-G	5.6, 10.4	S	S	S	S	S
MK-C	11.68	L	L	L	L	L
Acetaminophen	9.5	S	S	L	S	S
Ketoprofen	4.0-4.5	S	L	L	L	S
Indomethacin	4.5	S	S	S	S	S
Ketoconazole	2.9, 6.5	L	L	L	L	L
Itraconazole	3.7	S	S	L	S	S
MK-H	12.7	L	L	L	L	L
MK-J	3.3, 9.9, 13.8	S	S	L	S	S
MK- K	1.2, 3.2, 12.0	S	S	L	S	S
MK-L	4.5, 11.1, 12.7	S	S	S	S	S
MK-M	3.0, 9.4	S	S	S	S	S
MK-E	4.9, 13.6	L	L	L	L	L
MK-D	5.3, 7.5	S	S	L	S	S

L = Liquid; S = Solid

Glass Transition Temperature

The glass transition temperatures (T_g) after the first cycle of mDSC or the melting points are listed in Table 2 for all measured samples with the plots located in Appendices A and B, respectively. The T_g of the prepared lidocaine salicylate samples differ from the literature sample⁶. A likely reason is the different amounts of residual solvents and/or water in the samples, as discussed above. Water is a plasticizer for amorphous systems, which would explain why a system with more water, like batch 3 vs. 3b, would have a lower T_g . The literature sample of Propantheline tosylate has a T_g of 7°C, while the sample prepared in these experiments had a T_g of -4.5°C, a 11.5°C decrease. Like the Lidocaine salicylate, the differences in the T_g of the two samples may be related to differing levels of residual solvent in the systems. MK-B tosylate exhibits a 22°C glass transition and then a small endotherm at 90°C that may represent a heterogeneity in the sample or that the sample is becoming ordered upon heating, leading to a melting event. MK-E tosylate and citrate salts exhibit similar behavior upon heating. The tosylate salt has two glass transitions at 18.51°C and 41.76°C. The citrate salt has three at 22.31°C, 41.25°C, and 77.56°C. The MK-C tosylate and citrate salts as well as the ketoconazole mandelate and malate salts have glass transitions that are at or slightly above room temperature.

Table 2. Percent weight loss by 100°C (RS), Glass Transition Temperature (Tg) and Melting Points (Tm) of Attempted Active Ionic Liquids

Sample	RS (%)	Tg (°C)	Tm (°C)
Lidocaine Salicylate (1)	NM	14.30	
Lidocaine Salicylate (2)	0.1959	16.74	
Lidocaine Salicylate (3)	3.431	-11.66	
Lidocaine Salicylate (3b)	0.2691	-3.28	
Lidocaine Benzoate	0.9749	-22.92	
Lidocaine Malate	2.309	19.94	
Lidocaine Mandelate	0.5051	3.18	
Lidocaine Tosylate	0.366		150.76
Lidocaine Nicotinate	0.3228		59.95
Lidocaine Fumarate	0.2888		67.98
Propantheline Tosylate	0.8685	-4.51	
Tolfenamic Lysine	NM		212
Tolfenamic Lidocaine	NM		96
MK-A Glutamate	2.298		106.62
MK-A Mesylate	5.459		171.21
MK-A Acetate	NM		188.08
MK-A Salicylate	3.022		158.5
Piroxicam Citrate	NM		153.08
Piroxicam Tosylate	NM		114.06
MK-B Tosylate	4.285	21.95	89.98
MK-C Benzoate	0.6524	-5.8	
MK-C Malate	1.107	-26	
MK-C Tosylate	1.1245	20.21	
		71.47	
		9.96	
MK-C Mandelate	0.5529	75.96	
		18.21	
		59.54	
MK-C Citrate	0.2145	84.63	
MK-C Benzoate	0.6524	-5.8	
MK-C Malate	1.107	-26	
MK-C Tosylate	1.1245	20	
MK-C Mandelate	0.5529	10	
MK-C Citrate	0.2145	17	
Acetaminophen Tosylate	0.9585		122.7
Itraconazole Tosylate	0.5748		92.37
MK-D Tosylate	NM		111.19
Ketoconazole Malate	0.5838	23.40	
Ketoconazole Tosylate	0.5119	14.84	
Ketoconazole Mandelate	0.1919	31.60	
Ketoconazole Citrate	0.1648	11.86	

Ketoprofen Malate**	1.064	-6.02	
Ketoprofen Tosylate**	1.878		77.22
Ketoprofen Mandelate**	0.6161	-14.39	
MK-E Benzoate	0.6305	6.84	
MK-E Malate	1.322	7.97	
		18.51	
MK-E Tosylate	1.717	41.76	
MK-E Mandelate	1.047	6.88	
		22.31	
		41.25	
MK-E Citrate	0.8619	77.56	

NM = Not Measured

**Samples crystallized during of benchtop storage.

Viscosity

The viscous nature of the lidocaine salicylate, malate, and mandelate and propantheline tosylate were revealed through a series of rheometric studies at increasing temperatures. The viscosities of these samples tested are listed in Table 3, with additional data in Appendix E. Lidocaine salicylate is practically a solid at room temperature, with a viscosity of 8.05×10^5 Pa*s. A portion of sample stuck to the side of a round bottom flask would take several hours to flow to the bottom of the flask. The rheometry method was set so the plate rotated at increasing speed, from 0 to 500 rad/s. At 22°C, the plate rotation rate could only increase from 0 to 0.19 rad/s. When the temperature is increased to 40°C, the plate rotation rate only increased to 31 rad/s. The temperature had to be raised to 60°C for the plate to reach the desired 500 rad/s spin rate. Even at 60°C, the material has a viscosity of 81.6 Pa*s. At 80°C, the material thins to a flowable 5.4 Pa*s. For reference, honey has a reported viscosity of 2-10 Pa*s¹⁹. Lidocaine benzoate's viscosity is 28.76 Pa*s at 22°C and 3.09 Pa*s at 40°C. Lidocaine mandelate has a viscosity of 7280 Pa*s at 22°C and 8.2 Pa*s at 80°C. The malate salt is the most viscous lidocaine AIL made with a viscosity of 77.82 Pa*s at 80°C. The propantheline tosylate data tracks with the lidocaine

data except for the order of magnitude lower viscosity at 22 °C as compared to 40 °C. The cause of this anomaly is unknown.

Table 3. Viscosity at various temperatures for four Active Ionic Liquids

T (°C)	Viscosity (Pa*s)				
	Propantheline Tosylate	Lidocaine Malate	Lidocaine Mandelate	Lidocaine Salicylate	Lidocaine Benzoate
22	410.1	NM	7280	8.09E+05	28.76
40	5558	NM	129.1	4571	3.09
60	314.6	830.2	8.26	81.60	NM
80	19.27	77.82	NM	5.4	NM

NM = Not Measured

Fourier Transform Infrared Spectroscopy

Attenuated total reflectance Fourier transform infrared spectroscopy was used to analyze the ionic liquid samples and the parent compounds. The peak tables are listed in the Table 4. The spectra of lidocaine benzoate overlaid with its parent compounds is in Figure 2. All other spectra are in Appendix G.

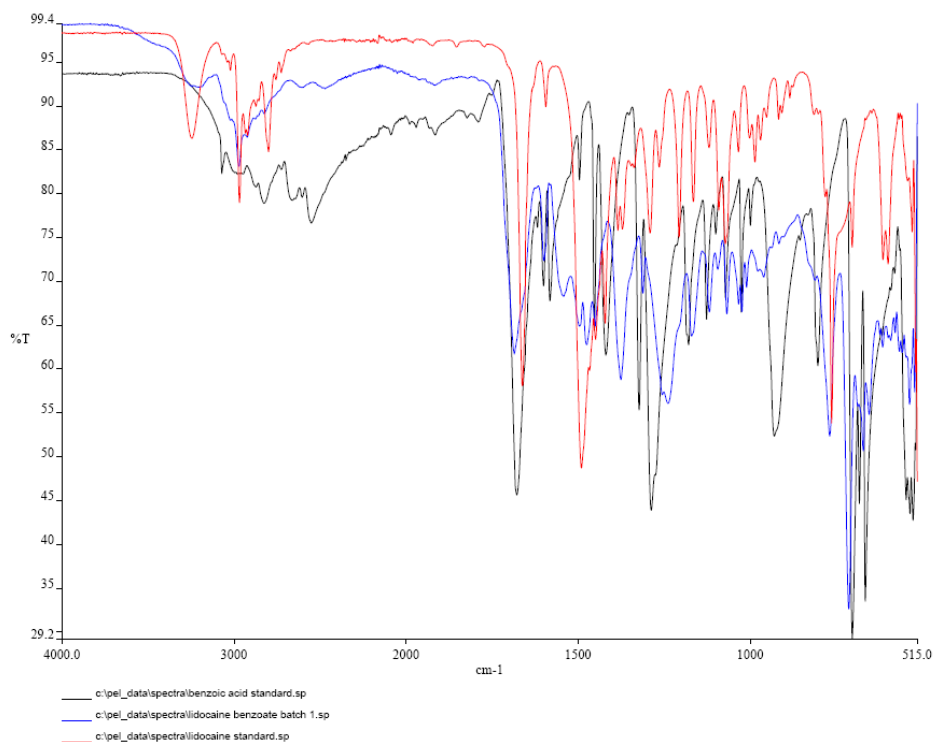


Figure 2. Lidocaine standard (red), Benzoic acid standard (black), and Lidocaine benzoate (blue) overlaid IR spectra.

Table 4. Identifying Peaks for Salt Formation of Lidocaine Ionic Liquids

Peak wave-number (cm ⁻¹)	Lidocaine	Lidocaine Salicylate		Lidocaine Benzoate		Lidocaine Mandelate		Lidocaine Malate	
		Salt	Acid	Salt	Acid	Salt	Acid	Salt	Acid
COOH			1655		1678		1705		1689
COO-		1626		1600		1600		1590	
COOH			1382		1419		1452		1410
COO-		1378		1376		1355		1375	
C-N stretch	1490								
C-N stretch ionized		1483		1475		1472		1471	
		1456		1449		1451		1420	

Nuclear Magnetic Resonance

The proton Nuclear Magnetic Resonance (^1H NMR) spectra are in Appendix D. The peak lists for lidocaine salicylate and propantheline tosylate compared to the literature values are below in Table 5. The spectra of lidocaine benzoate, malate and mandelate salts are the same as the parent spectra.

Table 5. ^1H NMR Spectra for Lidocaine Salicylate and Propantheline Tosylate

Lidocane Salicylate, ^1H NMR 400Hz	
Literature	Experimental
10.05 (br s 1H)	9.9 (br, s, 1H)
7.72 (dd, $J_1=7.75\text{Hz}$; $J_2=1.8\text{Hz}$, 1H)	7.72 (dd, 1H)
7.24 (m, 1H)	7.3 (m, 1H)
7.09 (s, 3H)	7.1 (s, 3or 4H)
6.70 (m, 2H)	6.7 (m, 2H)
3.98 (s, 2H)	3.9 (s, 2H)
3.10 (q, $J=7.28\text{Hz}$, 4H)	3.1 (q, 4H)
2.16 (s, 6H)	2.2 ((s, 6H)
1.22 (t, $J=7.34\text{Hz}$, 6H)	1.2 (t, 6H)

Propantheline Tosylate, ^1H NMR 400Hz	
Literature	Experimental
1.14-1.18 (t, 12H)	1.15-1.19 (t, 12H)
2.29 (s, 3H)	2.24 (s, 3H)
2.66 (s, 3H)	2.65 (s, 3H)
3.42-3.45 (t(b) 2H)	3.42 (t, 2H)
3.70-3.79 (m, 2H)	3.7-3.8 (m, 2H)
4.36-4.39 (t(b), 2H)	4.4 (t, 2H)
5.31 (s, 1H)	5.32 (s, 1H)
7.09-7.12 (m, 2H)	7.1-7.23 (m, 6H)
7.12-7.22 (m, 4H)	
7.39-7.40 (m, 4H)	7.35-7.5 (m, 6H)
7.46 - 7.49 (m, 2H)	

X-Ray Powder Diffraction

X-ray spectra overlays of lidocaine with the attempted tosylate, fumarate, and nicotinate salts revealed that salt formation did not take place because the product has the same XRD spectra as

the parent compound. The lidocaine nicotinate sample XRD pattern overlaid with lidocaine free base is in Figure 3. The XRD pattern overlays for the other listed samples are in Appendix F.

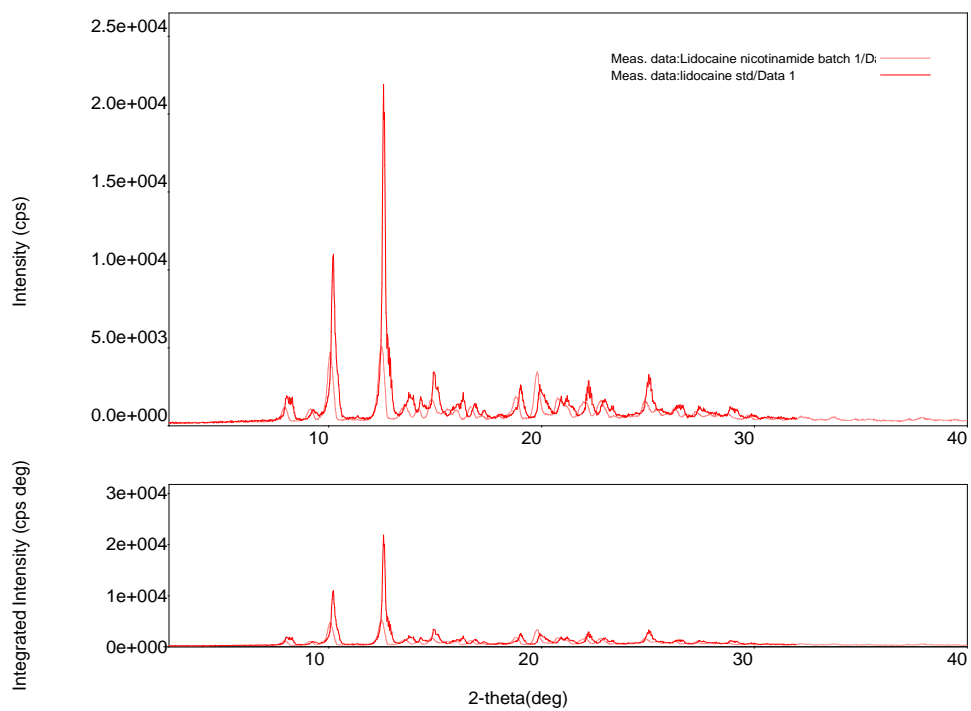


Figure 3. Lidocaine with nicotinic acid sample (pink) and lidocaine standard (red) XRD patterns.

Physical Stability

The lidocaine salicylate, benzoate, malate, and mandelate ionic liquids are physically stable for at least 20 months with benchtop storage. They are clear to slightly yellow in color. Merck C AILs are clear but the MK- E AILs are yellow colored. The Ketoconazole AILs are dark red but still transparent. MK-B, MK- C, MK- E, and Ketoconazole AILs are physically stable for at least 9 months. The ketoprofen salts crystallized after 1-3 weeks at benchtop conditions. The second endotherm of MK-B tosylate at 90°C is indicative of a crystallization risk, as are the heterogenous systems of MK-E tosylate and citrate.

Residual Solvent

TGA was used to determine total amount of RS remaining in the sample after vacuum drying. Without the attachment of a mass spectroscopy unit, the identity of solvent evaporating over time could not be determined. The amount of total solvent lost by 100°C after a 10°C/min ramp for all the samples tested is listed in Table 2. Samples prepared in a 4 mL or 20 mL round bottom flask were dried to less than 6% total solvent by heating under a vacuum. Further drying was not needed for the samples that were scale-ups from screen hits. By TGA analysis, 3.43 weight % of solvent was lost from the lidocaine salicylate sample 3 by 100°C, including acetone, water, and DCM. The water analysis by Karl Fisher titration determined that there was 2 % by weight absorbed by the sample. Analysis by gas chromatography detected 0.25 % by weight of acetone and dichloromethane. Adding the KF and GC solvent amounts together give a total solvent amount of 2.25 weight %, which is 1.18 % by weight lower than the total determined from TGA weight loss upon heating. As this sample is quite hygroscopic (see DVS results), the absorbed moisture may be a dynamic amount reflecting the ambient humidity of the sample storage conditions. Further drying at 5mBar (sample 3b) resulted in 0.26 % by weight lost upon heating to 100°C.

Hygroscopicity

The plots of humidity absorption/desorption of lidocaine salicylate, propanthline tosylate, and lidocaine benzoate are in Appendix C. Figure 4 is a plot of the lidocaine salicylate % by weight of water absorbed vs. time. The plot compares weight % vs time to relative humidity vs. time so that it is easily observable that the sample did not reach equilibrium between humidity increases. The sorption plot for Lidocaine Salicylate did not show significant water sorption until conditions greater than 80% RH. However, weight stabilization was not achieved within the

designated 180 min before the between humidity increases, suggesting that the sample may be more hygroscopic than the experimental conditions can determine. The water sorption data for propantheline tosylate was collected with a longer maximum dwell time of 360 min. The sorption plot is as expected for an AIL. Propantheline tosylate is a hygroscopic compound, gaining 5% by weight upon reaching 60% RH and over 20 % by weight upon reaching 95% RH. The water sorption is completely reversible upon dehumidification. Lidocaine benzoate is also highly hygroscopic. The reversible water adsorption of 30% by weight upon reaching 95% RH occurs mostly between 60% and 95% RH.

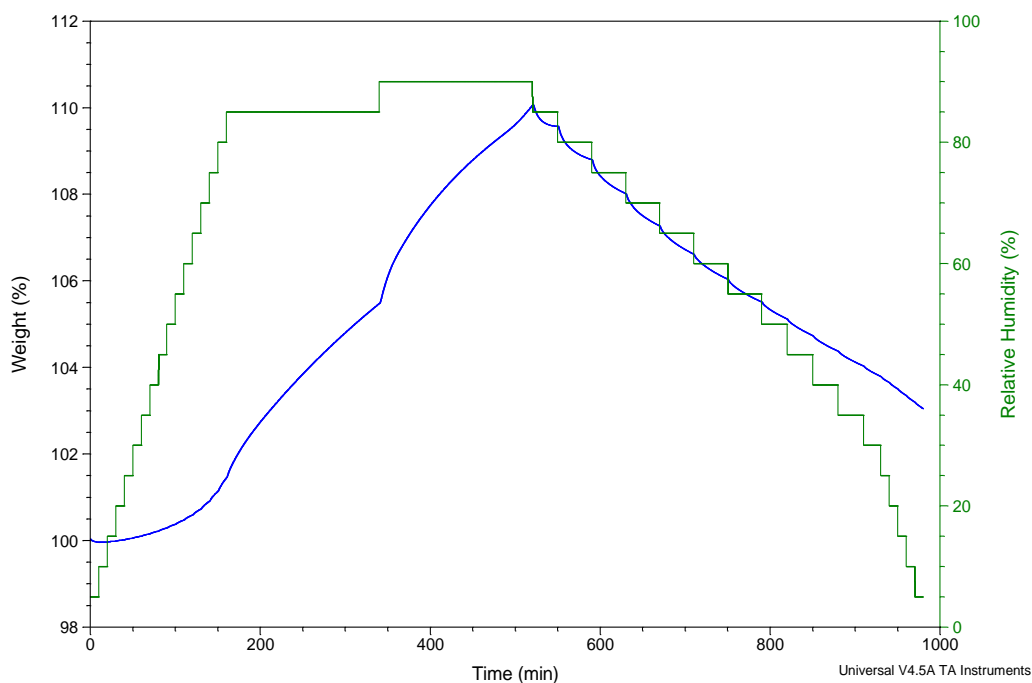


Figure 4. Plot of the percent weight gain by lidocaine salicylate batch 3b sample vs. time (blue line) and the measured relative humidity of the sample chamber vs. time (green line).

Salt Factor and Solubility

Twenty samples were tested for the percentage of parent compound in the sample and 15 of those samples had less than 10% difference in measured percentage and calculated for a mono-

salt, after correcting for residual solvent as measured by TGA. Five samples had a greater than 10% difference from the calculated mono-salt stoichiometry. All are listed in Table 6 with their aqueous and biorelevant solubilities.

Table 6. Salt Factor of ionic liquids and Solubility of ionic liquids compared to free form at 2 and 24 hours.

Sample	Vehicle	Salt Factor	Free base equivalents (mg/mL)	
			2 h	24 h (pH)
Lidocaine	Water		NM	NM (NM)
Lidocaine	SGF		NM	11.0* (NM)
Lidocaine	FaSSIF		NM	11.7* (NM)
Lidocaine	10% TW80		NM	24.6* (NM)
Lidocaine Salicylate	Water	1.57	55.6	27.4 (5.85)
Lidocaine Salicylate	SGF		57.5	34.8 (5.52)
Lidocaine Salicylate	FaSSIF		51.9	32.2 (5.8)
Lidocaine Salicylate	10% TW80		110	131 (5.79)
Lidocaine Benzoate	Water	1.62	51.8*	51.3* (5.91)
Lidocaine Benzoate	SGF		32.1*	31.7* (5.11)
Lidocaine Benzoate	FaSSIF		28.2*	29.8 (6.11)
Lidocaine Benzoate	10% TW80		67.0*	66.9* (6.08)
Lidocaine Malate	Water	1.70	43.5*	43.0* (4.14)
Lidocaine Malate	SGF		102*	103* (4.06)
Lidocaine Malate	FaSSIF		63.2*	60 (4.15)
Lidocaine Malate	10% TW80		129*	144* (4.16)
Lidocaine Mandelate	Water	1.18	49.7*	48.8* (5.19)
Lidocaine Mandelate	SGF		37.0*	34.9 (4.11)
Lidocaine Mandelate	FaSSIF		123*	133* (5.74)
Lidocaine Mandelate	10% TW80		51.7*	106* (5.38)
MK-C	Water		NM	NM (NM)
MK-C	SGF		NM	1.60* (NM)
MK-C	FaSSIF		NM	1.20* (NM)
MK-C	10% TW80		NM	20.0* (NM)
MK-C Malate	Water	1.36	1.56	1.41 (2.54)
MK-C Malate	SGF		1.39	1.21 (1.88)
MK-C Malate	FaSSIF		1.45	1.02 (2.92)
MK-C Malate	10% TW80		5.67	11.8 (2.84)
MK-C Mandelate	Water	1.31	1.24*	1.16 (3.02)
MK-C Mandelate	SGF		1.26*	1.15 (1.93)
MK-C Mandelate	FaSSIF		1.29*	0.95 (6.15)

MK-C Mandelate	10% TW80		11.0*	13.6* (3.2)
MK-C Citrate	Water	1.19	1.61	1.43 (2.32)
MK-C Citrate	SGF		1.44	1.3 (1.91)
MK-C Citrate	FaSSIF		1.48	1.37 (2.48)
MK-C Citrate	10% TW80		17.5	19 (2.53)
MK-C Tosylate	Water	10.61	0.921*	1.08 (2.37)
MK-C Tosylate	SGF		0.663*	0.75 (1.62)
MK-C Tosylate	FaSSIF		0.847*	0.81 (5.84)
MK-C Tosylate	10% TW80		2.03*	1.52 (2.4)
Ketoconazole Malate	Water	1.29	21.2	12.5 (3.49)
Ketoconazole Malate	SGF		16.4*	18.2 (3.4)
Ketoconazole Malate	FaSSIF		10.5	6.43 (3.55)
Ketoconazole Malate	10% TW80		25.7*	27.5 (3.81)
Ketoconazole Tosylate	Water	1.32	7.47*	6.86 (3.55)
Ketoconazole Tosylate	SGF		17.6	15.8 (3.2)
Ketoconazole Tosylate	FaSSIF		6.20	3.88 (3.65)
Ketoconazole Tosylate	10% TW80		34.7	34.7 (4.05)
Ketoconazole Mandelate	Water	1.26	12.1	9.56 (3.72)
Ketoconazole Mandelate	SGF		15.9	14.6 (3.73)
Ketoconazole Mandelate	FaSSIF		11.1	4.77 (3.82)
Ketoconazole Mandelate	10% TW80		35.7	41.4 (4.29)
Ketoconazole Citrate	Water	1.43	28.8*	21.2 (3.77)
Ketoconazole Citrate	SGF		25.6*	26.4* (3.66)
Ketoconazole Citrate	FaSSIF		23.4	20 (3.95)
Ketoconazole Citrate	10% TW80		28.3*	29.7* (3.87)
* Threshold Equilibrium Value NM = Not Measured				

Discussion

It is expected that a screen without a purification or assisted evaporation step would tend towards false positives as small amounts of residual solvent can have a major impact on solubility of these compounds. It was observed that in particular the p-toluenesulfonic acid when dispensed from a THF stock seemed to create more false positives than the acids in methanol stock. There

were eleven total tosylate hits and six of those compounds did not have a screen hit with any other acid. Only one of these tosylate hits were scaled up to produce a stable ionic liquid. In the future, it is suggested that the same solvent be used for all stock solutions to mitigate a bias in the screen results.

MK- C, an amorphous free base compound, resulted in successful scaled up hits for ionic liquids for almost every acid tested. This opens up a new opportunity for amorphous compounds, which can have physical properties that are difficult to control. A stable liquid salt may be used instead of developing a solid dispersion to stabilize the metastable amorphous phase. When considering that multiple AILs can be made with lidocaine and MK- C, there may be trends that if a single ionic liquid phase can be found for a compound, several are likely to form. This supports the literature claims of tunable physical properties based on the counterion⁵. The Tg's of the MK-C AILs compare as follows: malate < benzoate < mandelate < citrate < tosylate. All have a glass transition temperature that is less than room temperature, although the citrate and tosylate salts only just below.

The trend of malate, benzoate and mandelate producing lower Tg AILs than citrate and tosylate continues with MK-E. The Tg's for the malate, benzoate and mandelate salts are all about the same, but the citrate and tosylate salts have multiple Tg's with the lowest of each being at the edge of room temperature.

The lidocaine properties follow a similar trend. Lidocaine formed benzoate, malate and mandelate AILs, but a solid tosylate salt was formed with lidocaine (citrate was not tested).

Tosylate AILs were successfully formed with propantheline and ketoconazole, so the very low pKa acid is still relevant for AILs screening. Nicotinic acid is a carboxylic acid that is structurally similar to benzoic acid and mandelic acid, but with a substituted pyridine instead of a substituted phenyl ring. Its pKa is 3.4, which is almost exactly the same as mandelic acid, pKa 3.37. Both suggest that it should form an ionic liquid with lidocaine. However, nicotinic acid did not react with lidocaine via the melt procedure. A solvent-mediated method wherein the two parent compounds are fully dissolved may facilitate reaction. Similarly, the fumaric acid sample did not react with lidocaine. Fumaric acid is a reduced structure compared to malic acid with one unsaturation. A possible reason that it wouldn't form a salt with lidocaine is perhaps that the trans configuration is prohibitive to the steric arrangement needed for ionic bonding. The pKa of fumaric acid is 3.03 – slightly lower than malic acid's 3.46 pKa. Like with the nicotinic acid, performing the reaction under fully dissolved conditions may facilitate salt formation. The melting point of these two acids adds to this postulation. Nicotinic and fumaric acids both have melting points greater than 200°C, but benzoic, mandelic, and malic acid all have melting points in the between 110-130°C. The temperature of the reaction vessel never increased enough to melt the acid and commence salt formation. Therefore, there is potential that if the reaction was performed using the solvent extraction method for the lidocaine salicylate batch 3, that a salt would form, liquid or solid⁶. The dual active AIL attempt with lidocaine and tolafenamic acid resulted in crystals suspended in a viscous liquid. It may be that lidocaine formed a non-mono salt with the tolafenamic acid, so there was excess tolafenamic acid left to recrystallize. This reaction also warrants further process development.

Proton Transfer Identification

Several key articles have already discussed the changes in IR spectra in salicylic acid, benzoic acid, malic acid, mandelic acid and lidocaine upon salt formation²⁰⁻²⁶. The extent of carboxylate ionization in salicylic acid modulates both antisymmetrical and symmetrical stretching of the bonds²⁷. When protonated, the antisymmetrical peak of the carboxylate appears between 1650 cm⁻¹ and 1750 cm⁻¹. The salicylic acid sample measured as a reference is within that range at 1655 cm⁻¹. The lidocaine salicylate sample exhibits a carboxyl antisymmetric peak shift to 1626 cm⁻¹. This indicates that there is ionic character at this acidic group. Bica, et al.²⁸ used the lack of a shift at this peak to prove that they had made a lidocaine–fatty acid melted co-crystal instead of an ionic liquid²⁸. This peak has also been used as a key difference in the sodium salicylate vs. salicylic acid²². There the ionized carboxyl peak only shifted down about 8 cm⁻¹ from 1660 to 1652 cm⁻¹ upon salt formation. The symmetrical stretching of the carboxyl peak is also affected by the proton transfer in lidocaine salicylate²⁷. The peak shifts from 1382 cm⁻¹ in the acidic form to 1378 cm⁻¹ in the deprotonated state of the salt. The evidence for proton transfer is further enhanced by the lidocaine amide peak. In the free base spectrum, the carbonyl group of the amide has one peak at 1490 cm⁻¹, but in lidocaine salicylate, there are two peaks at 1486 cm⁻¹ and 1456 cm⁻¹. This was also observed in comparing lidocaine to its hydrochloride salt²¹. The peaks are attributed to the carbonyl group of the amide stretching. There are two bands in the salt form because the stretching is no longer equivalent in the two C-N bonds upon ionization. Based on the ionized carboxyl peak alone, lidocaine salicylate can be classified as an ionic liquid, with the other peak shifts serving as further support. IR can be used to identify the ionic nature of newly prepared liquid systems.

As all the successful lidocaine salt formations were with carboxylic acids, the peaks of interest are from the same functional groups as were analyzed for lidocaine salicylate. The lidocaine benzoate sample had the antisymmetric stretching carboxyl peak shift from 1678 cm^{-1} in the acidic form to 1600 cm^{-1} in the ionized form²³. Also, the symmetric stretching carboxyl peak shifted from 1419 cm^{-1} in the acidic parent to 1376 cm^{-1} in the ionized lidocaine salt. The carbonyl group of the amide in the lidocaine salt became the two peaks at 1475 and 1449 cm^{-1} , split from the single peak at 1490 in the lidocaine free base. These three shifts suggest that the proton from the carboxyl group of benzoic acid has transferred to the amide group in lidocaine, forming lidocaine benzoate salt.

The formation of the lidocaine mandelate salt can be supported by the antisymmetric stretching carboxyl peak shift from 1705 cm^{-1} in mandelic acid to 1600 cm^{-1} in the lidocaine salt^{24,26}. The corresponding symmetric stretching carboxyl peak shifted from 1452 cm^{-1} in mandelic acid to 1355 cm^{-1} in the lidocaine salt. The carbonyl group of the amide in the lidocaine salt became the two peaks at 1472 and 1451 cm^{-1} , split from the single peak at 1490 in the lidocaine free base. These three shifts suggest that the proton from the carboxyl group of mandelic acid has transferred to the tertiary amine group in lidocaine, forming lidocaine mandelate salt.

The lidocaine malate salt can be identified by the antisymmetric stretching carboxyl peak shift from 1689 cm^{-1} in malic acid to 1590 cm^{-1} in the lidocaine salt²⁵. The corresponding symmetric stretching carboxyl peak shifted from 1410 cm^{-1} in malic acid to 1375 cm^{-1} in the lidocaine salt. The carbonyl group of the amide in the lidocaine salt became the two peaks at 1471 and 1420 cm^{-1} , split from the single peak at 1490 cm^{-1} in the lidocaine free base. These three shifts suggest

that the lidocaine malate salt was formed by the proton from the carboxyl group of malic acid transferring to the tertiary amine group in lidocaine.

The NMR spectrum of lidocaine salicylate suggests that a material of the same composition as in Bica et.al was prepared⁶. The quaternary peak at 3.1 ppm corresponding to the four ethyl protons adjacent to the tertiary amine and the single peak at 3.9 ppm corresponding to the two methylene protons between the amide and the tertiary amine in the lidocaine salicylate sample are shifted to a higher frequency relative to the lidocaine sample, which has a corresponding quaternary peak at 2.6 ppm and a single peak at 3.2 ppm, respectively. The addition of a proton at this tertiary amine would produce a shift in peaks for these neighboring protons. There is a shift in the phenyl proton ortho to the carboxylic acid in salicylic acid when that carboxylic acid ionizes. The multi-peak for the single hydrogen is located at 7.5 ppm when the carboxylate is acidic. Once ionized, the peak shifted to 7.3 ppm for lidocaine salicylate. The NMR data compliments the IR data in pointing to a proton transfer from the carboxylic acid in salicylic acid to the tertiary amine in lidocaine forming an ionic salt.

The NMR spectral data of the Propantheline tosylate sample matched the literature data and indicated that the sample was not a physical mixture of the two starting components¹. It was also essentially identical to the Propantheline bromide starting material. The tosylate's phenyl protons are not apparent in the ionic liquid spectra. The NMR spectra of the other three lidocaine ionic liquids did not show shifts from the lidocaine free base spectra. The samples are dissolved in d⁶-DMSO, potentially disproportionating the salt. Rogers showed the same occurrence with lidocaine oleate ionic liquids. Only when the sample was measured using solid state NMR at a

temperature of 80° C did shifts become evident²⁹. Solution state proton NMR is therefore, not a robust method of confirming salt formation. Other techniques that maintain the phase of the material are better suited for AIL characterization. NMR can be utilized to determine purity of AIL samples¹². Solvents and unwanted reaction byproducts may be detected in the spectra, indicating further purification is needed.

Residual Solvent

The amount and identity of residual solvents in an active ionic liquid sample could have repercussions on a number of properties. The discrepancy between KF and TGA residual solvent amounts in the lidocaine salicylate sample may be due to the viscous nature of the sample causing solvent to become trapped within the liquid; and therefore, more slowly vaporized by the increasing temperatures in the TGA. Instead of a standard temperature ramp method for the TGA, an isothermal hold at an elevated temperature until the weight stabilizes would provide a rate and total amount of solvent loss without nearing the decomposition temperature. Karl Fisher titration for water is a better method, but not available on a routine basis. Assuming the solvent is water, it may play an important role in the physical properties of the liquid. It is a common occurrence that solvent impurities lower the glass transition temperatures of material³. The residual solvent would also manifest itself in the higher viscosity of the mandelate and malate salts of lidocaine over the benzoate salt. Mandelic acid and malic acid have increasing numbers of hydrogen bonding sites over benzoic acid. Mandelic acid has an additional hydroxy group and malic acid has two carboxylic acids and a hydroxyl group available for hydrogen bonding. Hydrogen bonding may be why the ketoprofen malate, mandelate, and tosylate samples were metastable in

the liquid phase. H-bonding between the two acids and the solvent may facilitate the liquid phase stability until the solvent evaporates fully.

A remaining issue is how to keep AIL samples dry during storage and during further experimental preparations. Dessicated storage is feasible but once the container is opened to atmospheric moisture how does one remove the absorbed water to maintain a consistent dryness over time? It is more practical to dry as much as possible during preparation and then account for the remaining water in subsequent characterization. If new experiments are conducted weeks/months after the initial TGA, then that assay may need to be re-run. When using solvent extraction instead of a melt reaction, then the weight loss in the TGA cannot be assumed to be only water. GC and KF analysis would need to be conducted to quantify the amount of solvent and water present in the sample.

The viscosity doesn't trend with glass transition, as well as expected. Lidocaine malate and malate ionic liquids have the same glass transition temperature of 3.3 and 3.2 °C, respectively. The viscosity of the malate salt at room temperature is an order of magnitude higher than the malate salt. The residual solvent may be affecting the viscosity. The malate salt has about three times the amount of residual solvent by TGA as the malate salt. The plasticizing affect of the solvent may influence the viscosity to a higher degree than the Tg. An issue lies in the dispensing of AILS. Even the least viscous lidocaine benzoate is difficult to handle at room temperature or in the molten state. The cohesivity of the liquid, (stickiness) can be compared again to honey. Regular or ad hoc dispensing of the compound is not practical and heated dispensing and mixing equipment is likely to be needed. An issue with slow mobility was apparent in the DVS data,

similar to the TGA results. The sorption plot for Lidocaine salicylate did not show significant water sorption until conditions greater than 80% RH (Figure 2). However, weight stabilization was not achieved within the designated 180 min before the between humidity increases, suggesting that the sample may be more hygroscopic than the experimental conditions can determine. The sample needs to be held at each humidity level for longer periods of time to better determine the hygroscopicity.

Salt Factor

The salt factor of the samples was determined by an HPLC analysis of the area of the parent active compound versus the area of the parent in the salt form. All the samples were prepared with equal-molar amounts of parent and counterion. Only the Propantheline tosylate sample was isolated with a filtration step to remove impurities and the silver bromide salt. The other samples do not have a purification step to remove excess reagents, which will then contribute to the total area of the parent or counterion in the HPLC assay. The assay should determine that all samples, with the possible exception of Propantheline tosylate are mono-salts, regardless of the actual stoichiometry. A case where the assay would be in error would be if the excess acid or base was soluble in the few percentage of solvent remaining in the sample or soluble in the ionic liquid itself. Ionic liquids were used as solvents for a number of years⁴. Literature references have shown that ionic liquids can be formed with greater than molar equivalents of active and therefore, presumably counterion³⁰.

Lidocaine mandelate's assay value corresponds to a hemi-salt. Two active ions share one proton. Based on the preceding discussion on the limitations of the assay, it is unknown exactly how this

result corresponds to the expected outcomes of the reaction. The most likely scenario is a weighing error during sample preparation, but was not confirmed through re-synthesis. Since the IR data supports proton transfer, an orthogonal method for accurately determining stoichiometry of the salt is needed. Propantheline tosylate is measured to be between a mono and a bis-salt. Based on the included filtration step in preparing this sample, incomplete filtration is likely the issue, with excess tosylate remaining in the sample. A possible confirmation experiment for this sample would be a sulfur-based elemental analysis assay. MK-A tosylate salt has a low area count for the parent compound. Degradation was not noted in the assay. A sample weight error is the likely cause of the low area, which then caused the percentage of parent in the sample to be in order of magnitude different than the calculated percentage for a mono-salt. MK-A citrate has a percentage of parent compound in the sample that more closely corresponds to a hemi-salt than a mono-salt. Ketoprofen mandelate has 11% error between the measured and calculated parent percentage in the sample, corresponding to the non-ionic nature of the bonding for this metastable liquid.

Solubility

Significant solubility increases of the AIL over their free base solubility was not observed for all samples. The solubility of the lidocaine ionic liquids did increase in aqueous media compared to the free base. In FaSSIF, the solubility increased from 11.7 mg/mL as the free base to 32.2 mg/mL as the salicylate salt ionic liquid, while maintaining the ionic liquid phase. Solubility was not increased in the MK-A ionic liquids when compared to free base. They likely disproportionated to the parent form, though this was untested. Ketoconazole free base solubility is needed to determine if there are differences upon liquid salt formation.

Conclusion

A medium throughput screen was developed for the formation of active ioninc liquids. The reproducibility of the hits upon scale up was typical for phase screening. The addition of more counterions and active compounds to the data set is needed, but proof of concept has been established. AILs can be screened by the same methods as conventional crystalline salts. Hopefully the “oil” wells in existing high throughput salt screens will not be rejected, but scaled up as potential AILs. Identification via IR and analysis of glass transition, residual solvent, salt factor and biorelevant solubility were conducted for a number of novel AILs of generic and propriatary compounds. While the equilibrium solubility enhancement of AILs over their neutral forms was not as high as hoped for, the kinetic advantage and utility for liquid dosing remains to be investigated. Ultimately, until preclinical species in vivo exposure data of an AIL is compared to the crystalline salt form and a collection of high POS ions is determined, the actual utility of AILs to drug development cannot be determined.

References

1. Dean PM, Turanjanin J, Yoshizawa-Fujita M, MacFarlane DR, Scott JL 2009. Exploring an Anti-Crystal Engineering Approach to the Preparation of Pharmaceutically Active Ionic Liquids. *Cryst Growth Des* 9(2):1137-1145.
2. Stoimenovski J, MacFarlane DR, Bica K, Rogers RD 2010. Crystalline vs. Ionic Liquid Salt Forms of Active Pharmaceutical Ingredients: A Position Paper. *Pharm Res* 27(4):521-526.
3. Murdande SB, Pikal MJ, Shanker RM, Bogner RH 2011. Solubility advantage of amorphous pharmaceuticals, part 3: Is maximum solubility advantage experimentally attainable and sustainable?. *J Pharm Sci* 100(10):4349-4356.
4. Hough WL, Rogers RD 2007. Ionic liquids then and now: from solvents to materials to active pharmaceutical ingredients. *Bull Chem Soc Jpn* 80(12):2262-2269.
5. Hough-Troutman WL, Smiglak M, Griffin S, Matthew Reichert W, Mirska I, Jodynis-Liebert J, Adamska T, Nawrot J, Stasiewicz M, Rogers RD, Pernak J 2009. Ionic liquids with dual biological function: sweet and anti-microbial, hydrophobic quaternary ammonium-based salts. *New Journal of Chemistry*
New J Chem 33(1):26-33.
6. Bica K, Rijksen C, Nieuwenhuyzen M, Rogers RD 2010. In search of pure liquid salt forms of aspirin: ionic liquid approaches with acetylsalicylic acid and salicylic acid. *Physical Chemistry Chemical Physics*
Phys Chem Chem Phys 12(8):2011-2017.
7. MacFarlane DR, Seddon KR 2007. Ionic liquids - Progress on the fundamental issues. *Aust J Chem* 60(1):3-5.
8. Angell CA 2002. Origin and control of low-melting behavior in salts, polysalts, salt solvates, and glassformers. *NATO Sci Ser, II 52(Molten Salts: From Fundamentals to Applications)*:305-320.
9. Krossing I, Slattey JM, Daguenet C, Dyson PJ, Oleinikova A, Weingaertner H 2007. Why are ionic liquids liquid? A simple explanation based on lattice and solvation energies. [Erratum to document cited in CA145:512046]. *Journal of the American Chemical Society* 129(36):11296.
10. Mudring A-V 2010. Solidification of Ionic Liquids: Theory and Techniques. *Aust J Chem* 63(4):544-564.
11. Mathias NR, Hussain MA 2009. Non-invasive systemic drug delivery: Developability considerations for alternate routes of administration. *J Pharm Sci* 99(1):1-20.
12. Clare B, Sirwardana A, MacFarlane DR 2009. Synthesis, purification and characterization of ionic liquids. *Top Curr Chem* 290(Ionic Liquids):1-40.
13. Bica K, Rodriguez H, Gurau G, Cojocaru OA, Riisager A, Fehrmann R, Rogers RD 2012. Pharmaceutically active ionic liquids with solids handling, enhanced thermal stability, and fast release. *Chem Commun (Camb)* 48(44):5422-5424.
14. Ferraz R, Branco LC, Marrucho IM, Araujo JMM, Rebelo LPN, da P, Manuel Nunes, Prudencio C, Noronha JP, Petrovski Z 2012. Development of novel ionic liquids based on ampicillin. *MedChemComm* 3(4):494-497.
15. Stahl PHCGW. 2011. *Pharmaceutical Salts: Properties, Selection, and Use*. 2 ed., Zurich: Wiley-VHC. p 388.

16. Black SN, Collier EA, Davey RJ, Roberts RJ 2007. Structure, solubility, screening, and synthesis of molecular salts. *J Pharm Sci* 96(5):1053-1068.
17. Serajuddin ATM 2007. Salt formation to improve drug solubility. *Adv Drug Delivery Rev* 59(7):603-616.
18. Pibiri I, Pace A, Buscemi S, Causin V, Rastrelli F, Saielli G 2012. Oxadiazolyl-pyridines and perfluoroalkyl-carboxylic acids as building blocks for protic ionic liquids: crossing the thin line between ionic and hydrogen bonded materials. *Physical Chemistry Chemical Physics Phys Chem Chem Phys* 14(41):14306-14314.
19. Elert G. 1998-2012. *The Physics Hypertextbook*. ed.
20. Neville GA, Regnier ZR 1969. Hydrogen bonding in lidocaine salts. I. NH stretching band and its dependence on the associated anion. *Can J Chem* 47(22):4229-4235.
21. Abu-Huwajj R, Assaf S, Salem M, Sallam A 2007. Mucoadhesive Dosage form of Lidocaine Hydrochloride: I. Mucoadhesive and Physicochemical Characterization. *Drug Dev Ind Pharm* 33(8):855-864.
22. Philip D, John A, Panicker CY, Varghese HT 2001. FT-Raman, FT-IR and surface enhanced Raman scattering spectra of sodium salicylate. *Spectrochim Acta, Part A* 57A(8):1561-1566.
23. Brittain HG 2009. *Vibrational Spectroscopic Studies of Cocrystals and Salts*. 2. The Benzylamine-Benzonic Acid System. *Cryst Growth Des* 9(8):3497-3503.
24. Badawi HM, Foerner W 2011. Analysis of the infrared and Raman spectra of phenylacetic acid and mandelic (2-hydroxy-2-phenylacetic) acid. *Spectrochim Acta, Part A* 78A(3):1162-1167.
25. Max J-J, Chapados C 2004. Infrared Spectroscopy of Aqueous Carboxylic Acids: Comparison between Different Acids and Their Salts. *J Phys Chem A* 108(16):3324-3337.
26. Gomes DJC, Caires FJ, Lima LS, Gigante AC, Ionashiro M 2012. Thermal behaviour of mandelic acid, sodium mandelate and its compounds with some bivalent transition metal ions. *Thermochim Acta* 533:16-21.
27. Wade LG, Jr. 2003. *Organic Chemistry*. 5 ed., Upper Saddle River, NJ: Pearson Education, Inc. p 1220.
28. Bica K, Shamshina J, Hough WL, MacFarlane DR, Rogers RD 2011. Liquid forms of pharmaceutical co-crystals: exploring the boundaries of salt formation. *Chem Commun (Cambridge, U K)* 47(8):2267-2269.
29. Rogers RD. 2011. *The Evolution of Ionic Liquids - From Solvents and Separations to Advanced Materials and Pharmaceuticals: Examples from the Ionic Liquid Cookbook*. ed., Tuscaloosa, AL.
30. Bica K, Rogers RD 2010. Confused ionic liquid ions--a "liquification" and dosage strategy for pharmaceutically active salts. *Chem Commun (Camb)* 46(8):1215-1217.

Appendix A: Thermogravimetric Analysis (TGA)

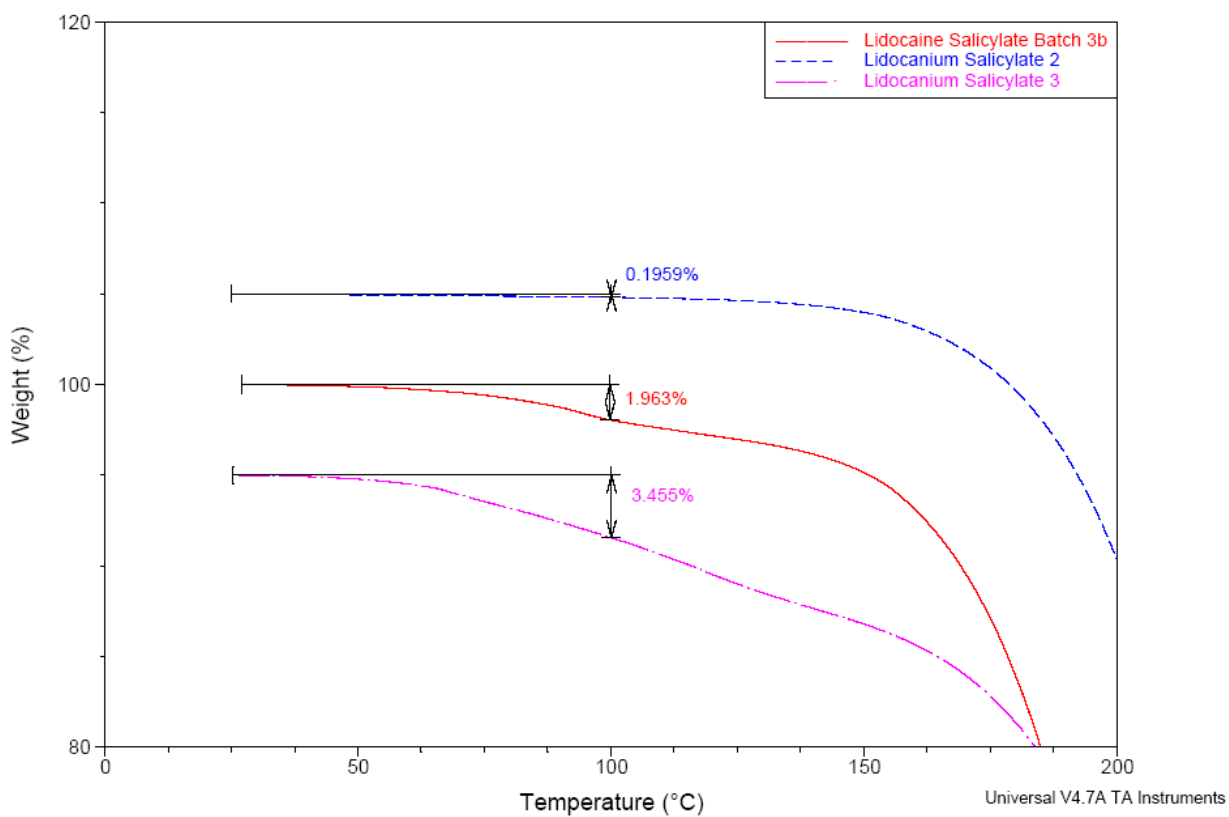


Figure A1. Lidocaine salicylate batches 2, 3, and 3b TGA spectra overlay.

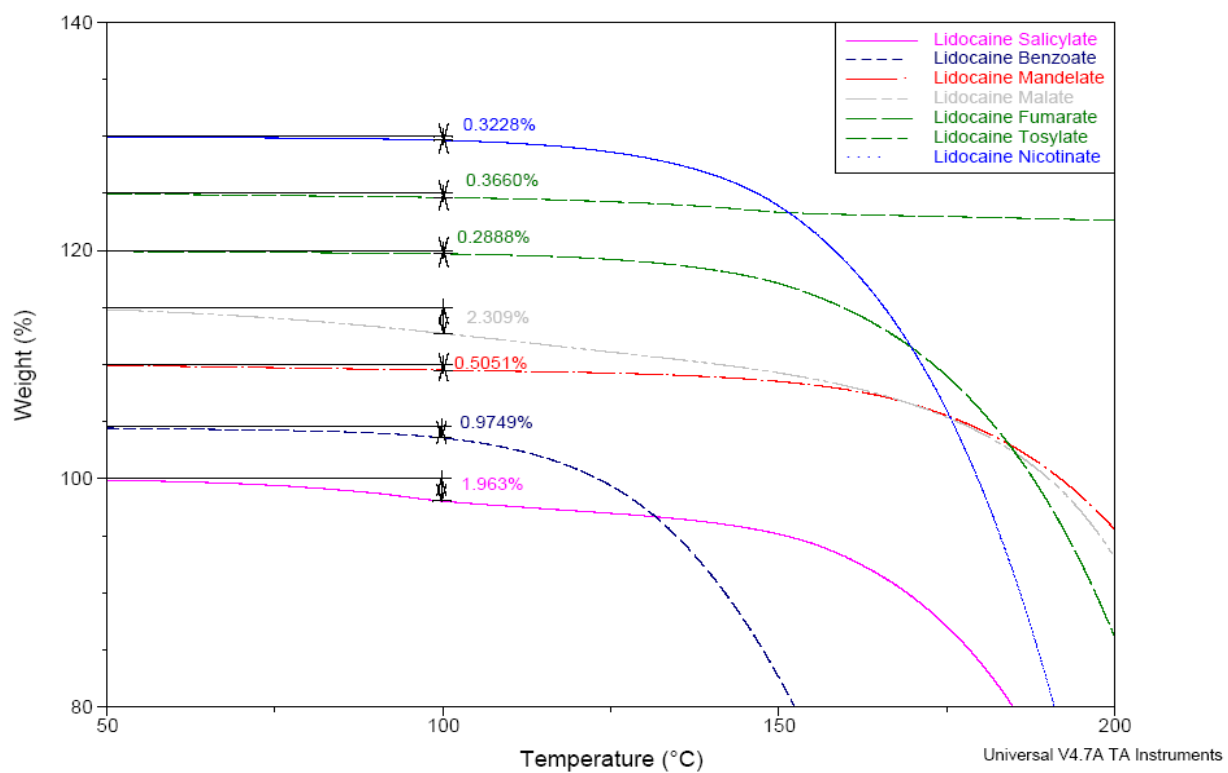


Figure A2. Lidocaine salicylate (3b), benzoate, mandelate, malate, fumarate, tosylate, and nicotinate TGA spectra overlay.

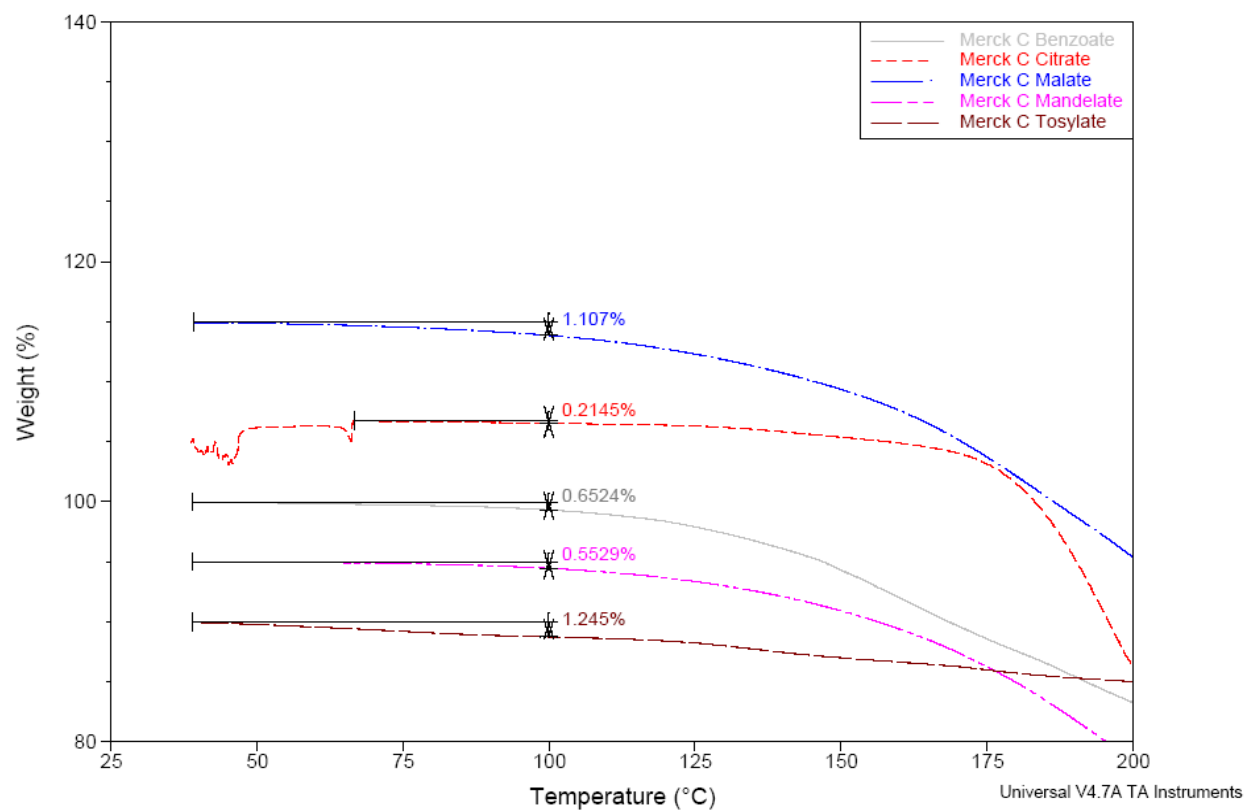


Figure A3. MK- C tosylate, mandelate, malate, citrate, and benzoate TGA spectra overlay.

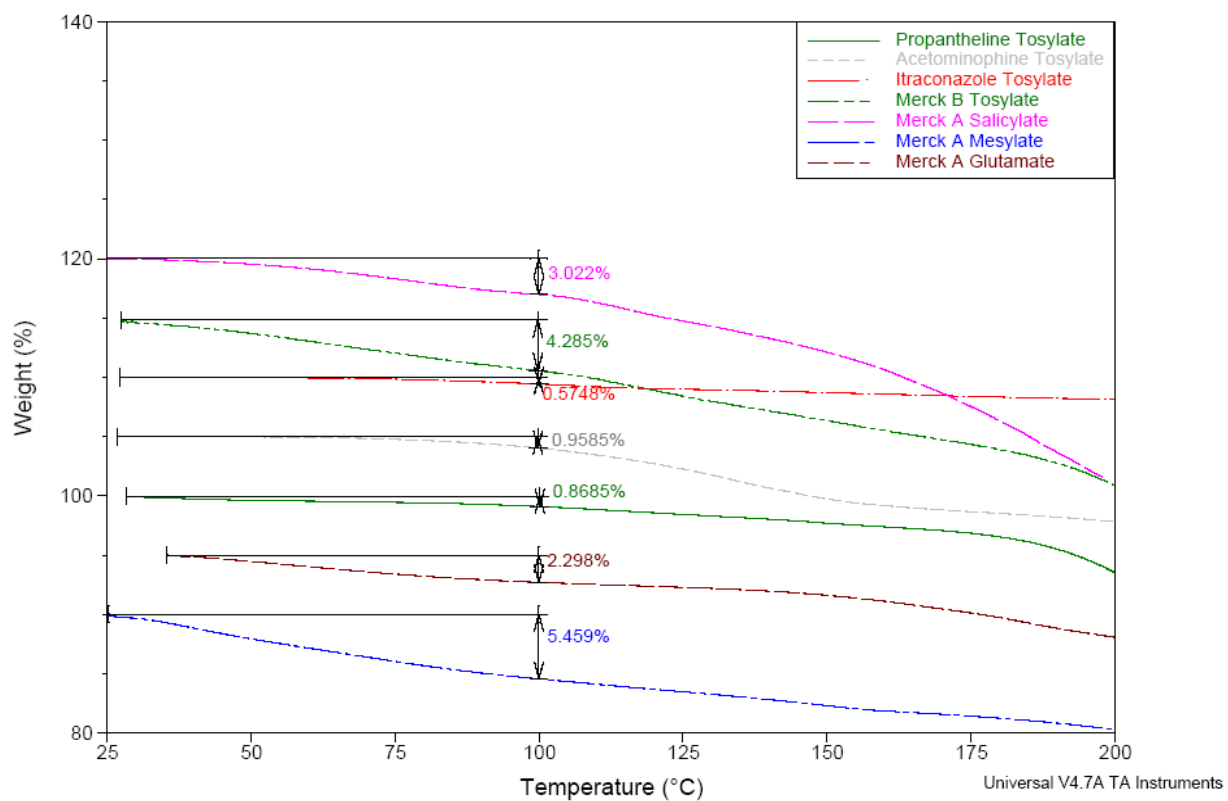


Figure A4. MK- A glutamate, MK- A mesylate, MK- A salicylate, MK-B tosylate, Itraconazole tosylate, Acetaminophine tosylate, and Propantheline tosylate TGA spectra overlay.

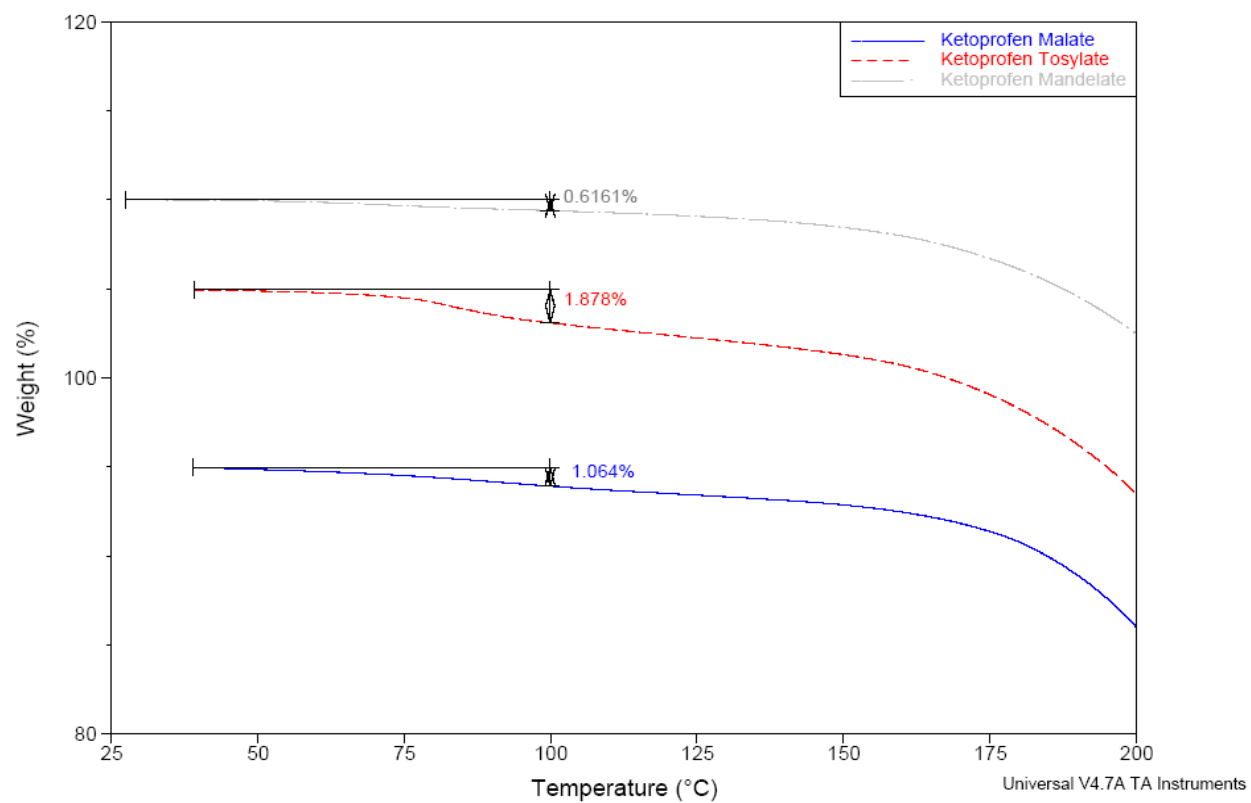


Figure A5. Ketoprofen malate, tosylate, and mandelate TGA spectra overlay.

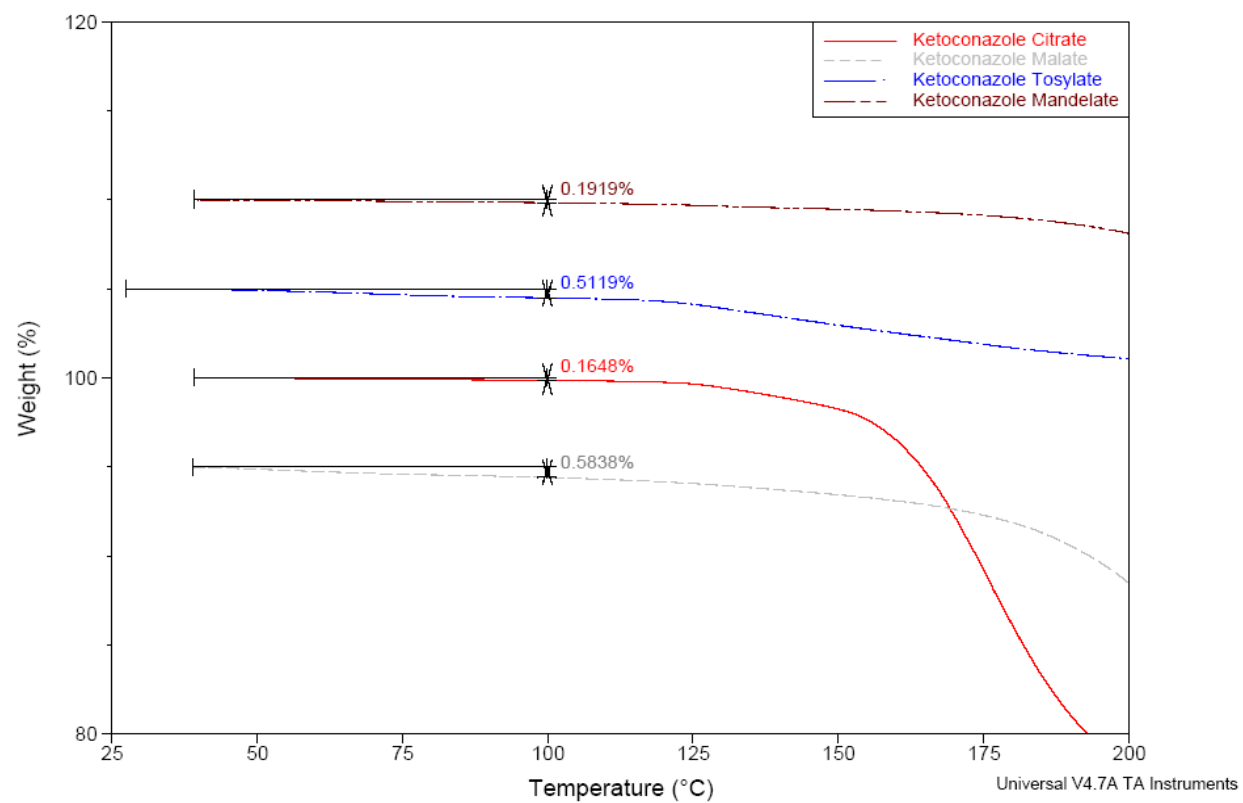


Figure A6. Ketoconazole citrate, malate, tosylate, and mandelate TGA spectra overlay.

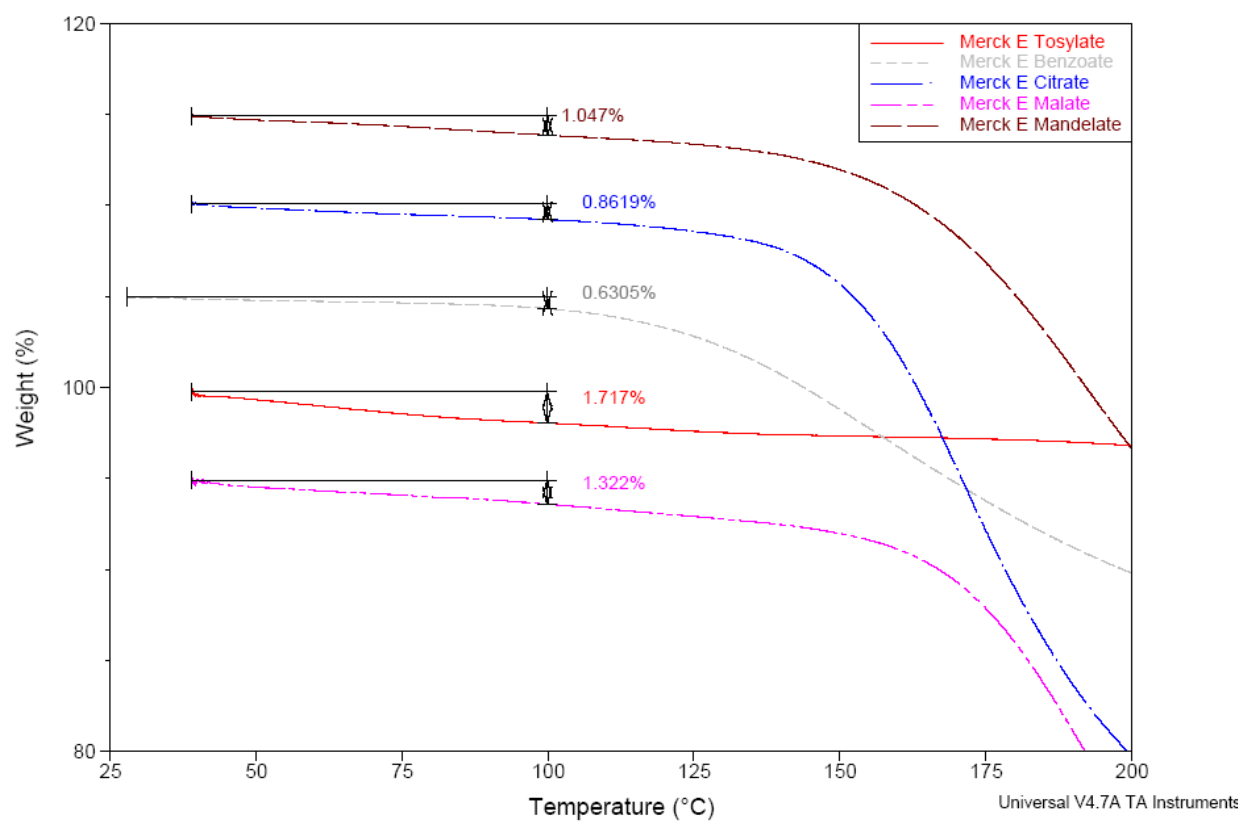


Figure A7. MK- E tosylate, benzoate, citrate, malate, and mandelate TGA spectra overlay.

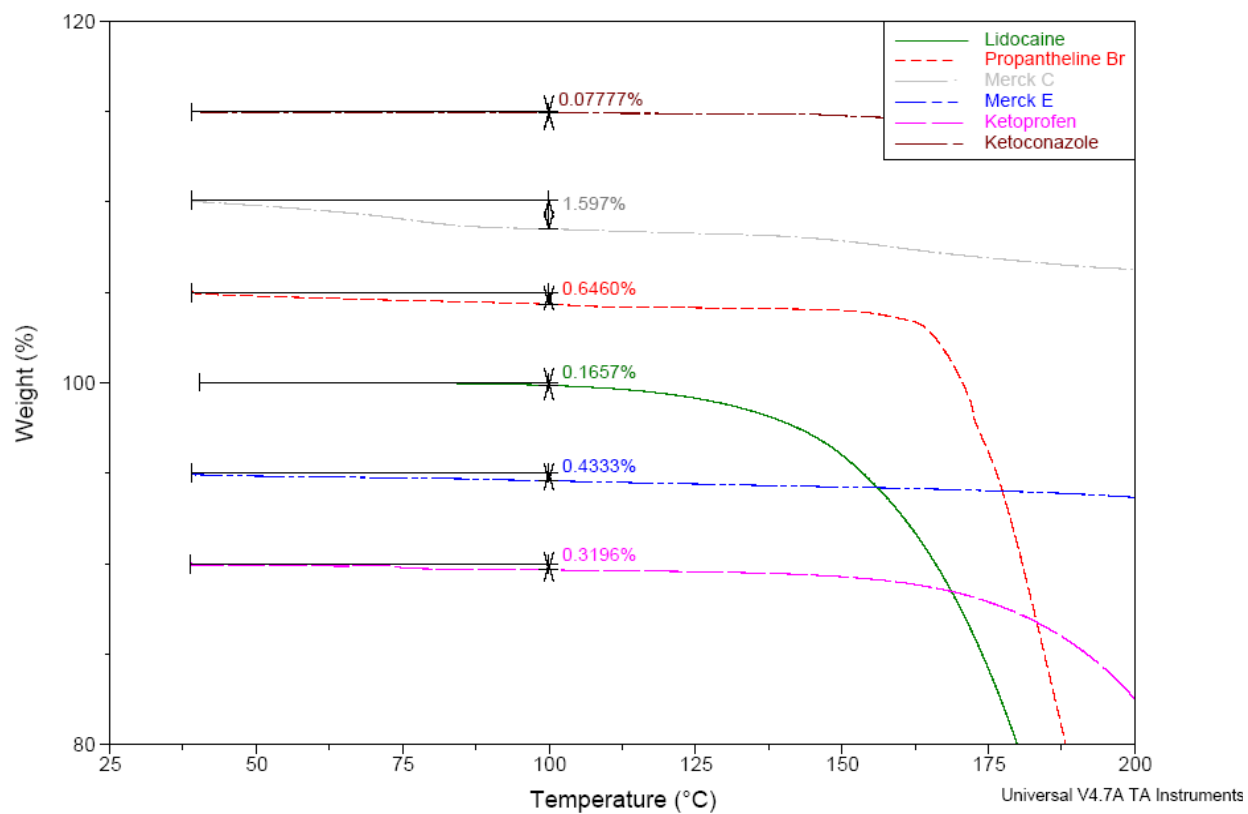


Figure A8. Lidocaine, Propantheline Br, Merck C, Merck E, Ketoprofen and Ketoconazole parent compound standard TGA spectra overaly.

Appendix B: Modulated Differential Scanning Calorimetry (mDSC)

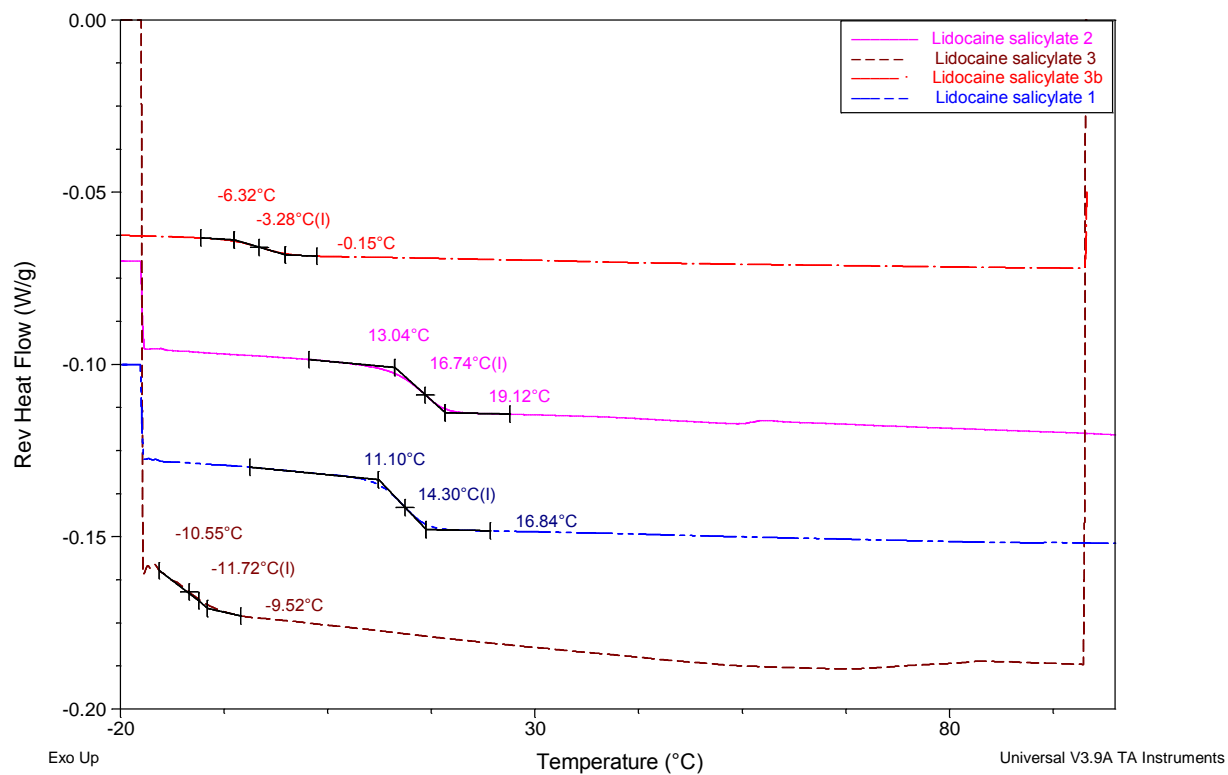


Figure B1. Lidocainium salicylate batch 1 (blue), batch 2 (pink), batch 3 (maroon) and batch 3b (red) mDSC overlay with cycle 1 glass transition temperature indicated.

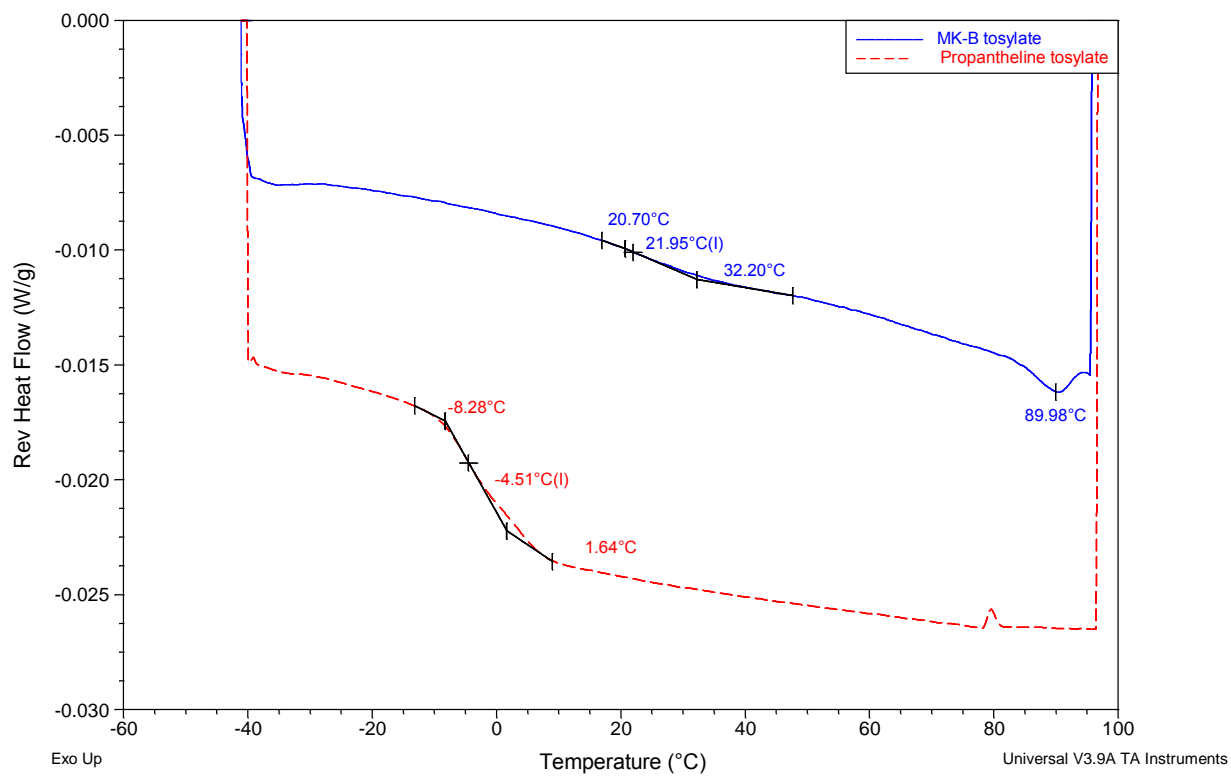


Figure B2. Propantheline tosylate (red) and MK-B tosylate (blue) mDSC overlay with cycle 1 glass transition temperature indicated.

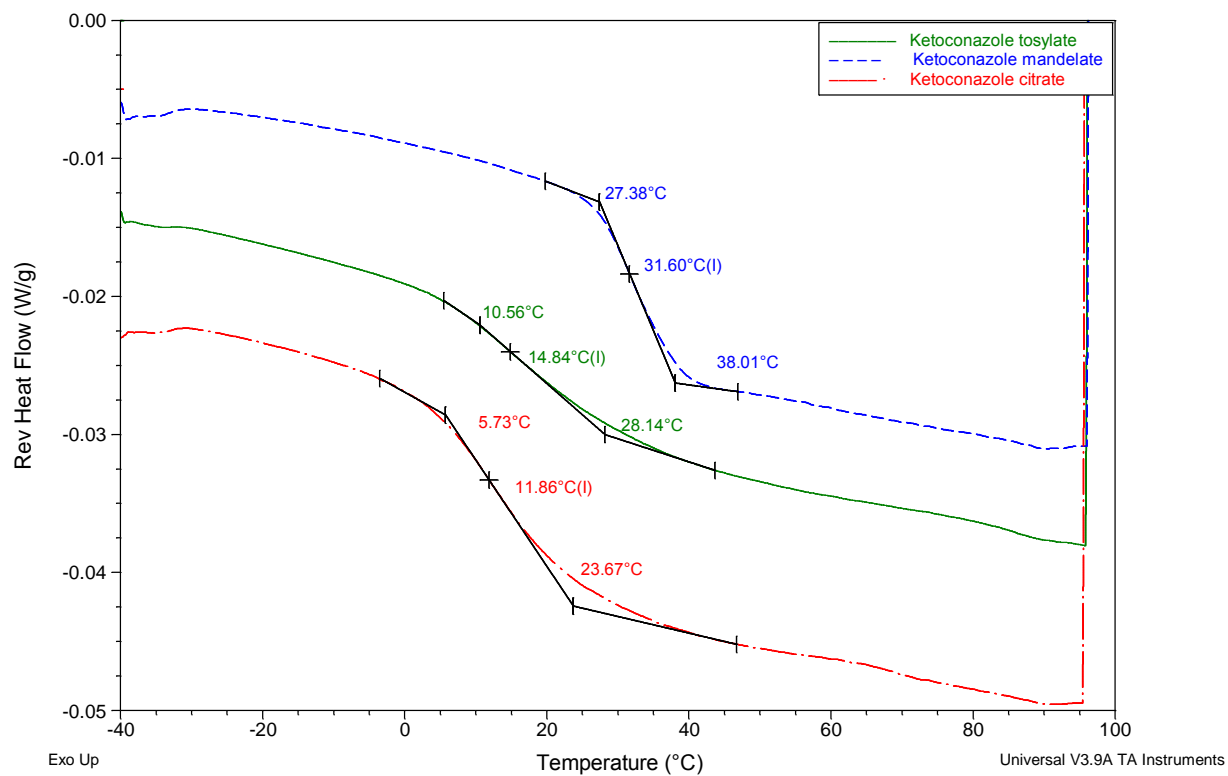


Figure B3. Ketoconazole tosylate (green), ketoconazole mandelate (blue), and ketoconazole citrate (red) mDSC overlay with cycle 1 glass transition temperature indicated.

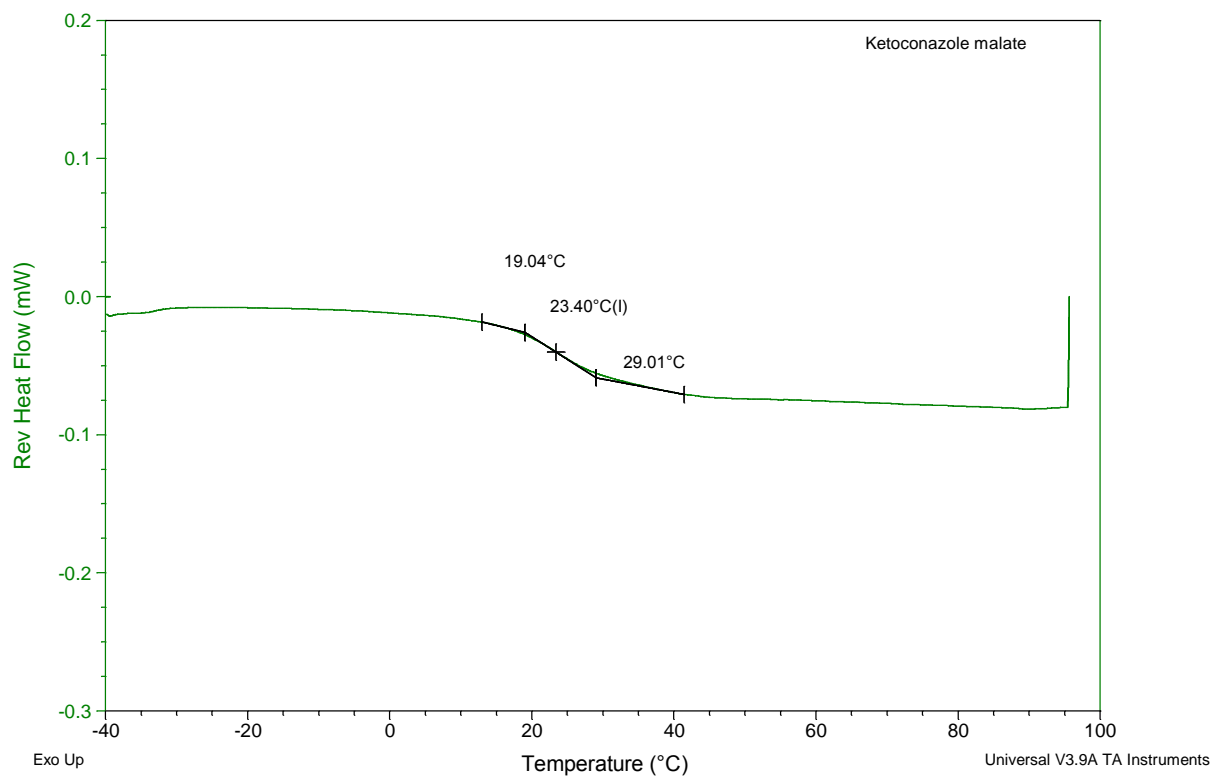


Figure B4. Ketoconazole malate mDSC with cycle 1 glass transition temperature indicated.

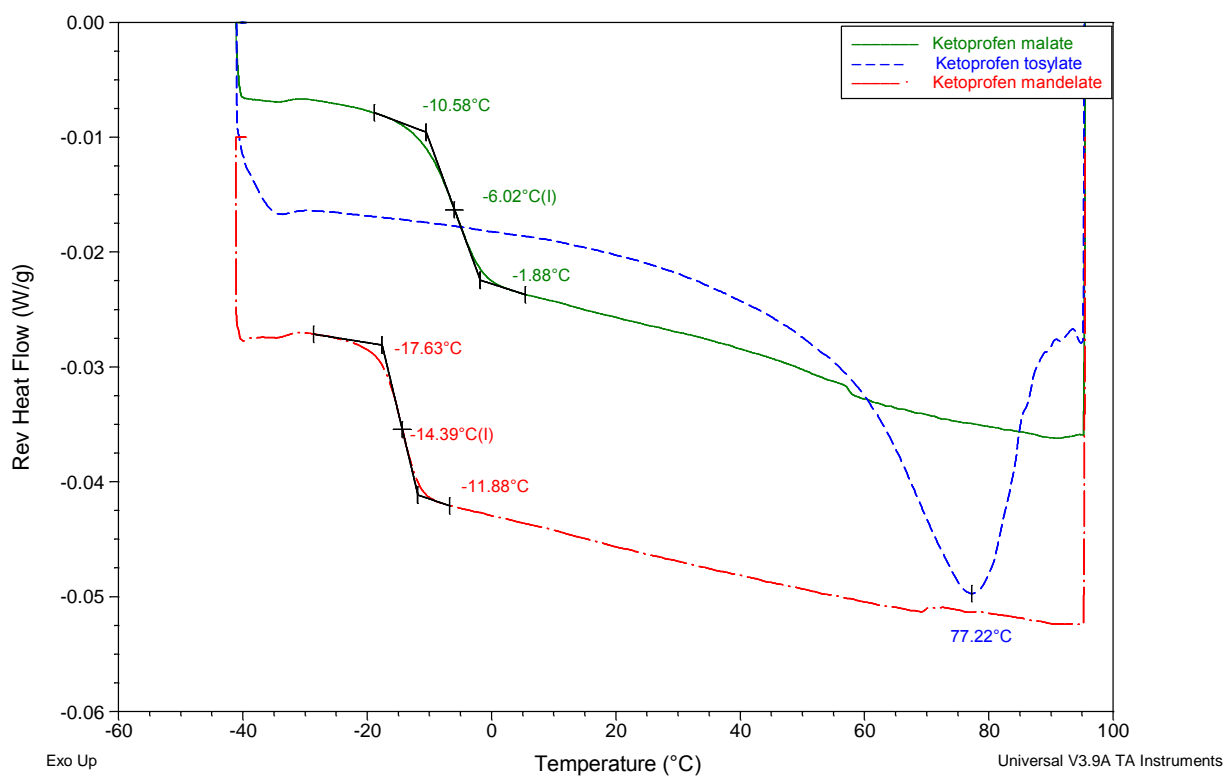


Figure B5. Ketoprofen malate (green), tosylate (blue) and mandelate (red) mDSC overlay with cycle 1 glass transition temperature indicated.

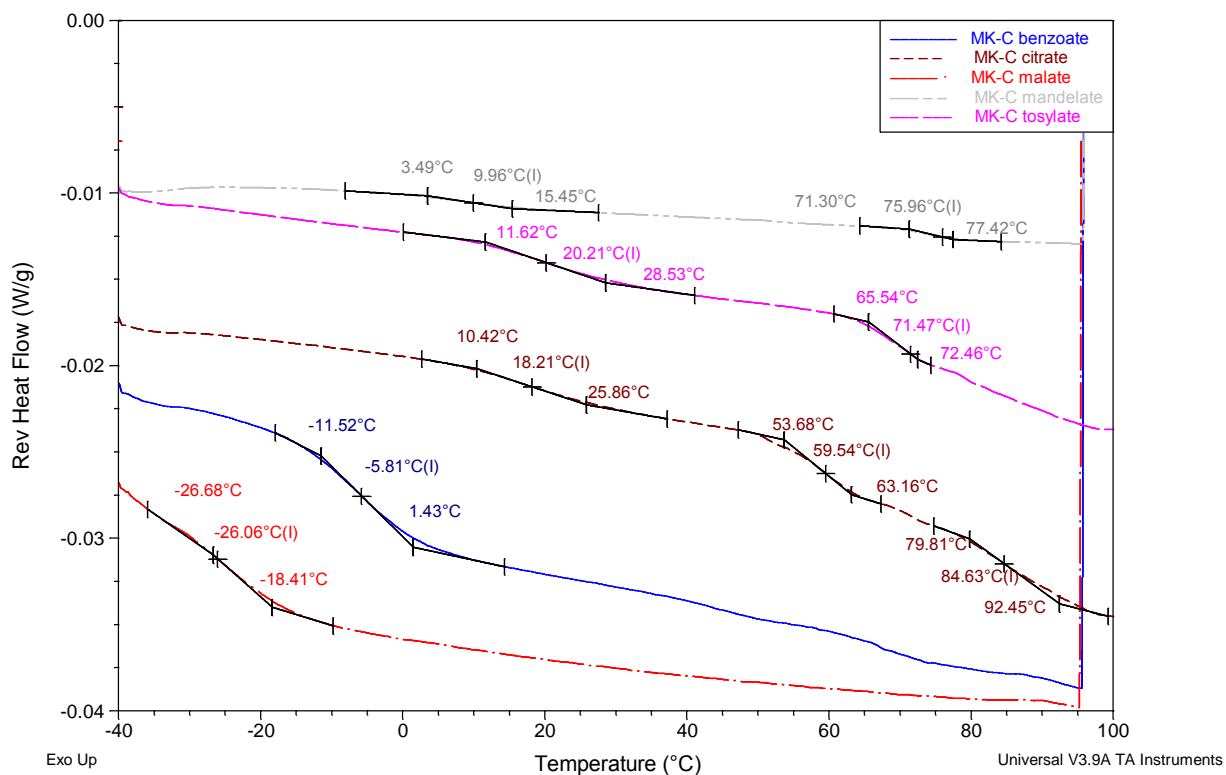


Figure B6. MK-C benzoate (blue), citrate (maroon), malate (red), mandelate (silver), and tosylate (pink) mDSC overlay with cycle 1 glass transition temperature indicated.

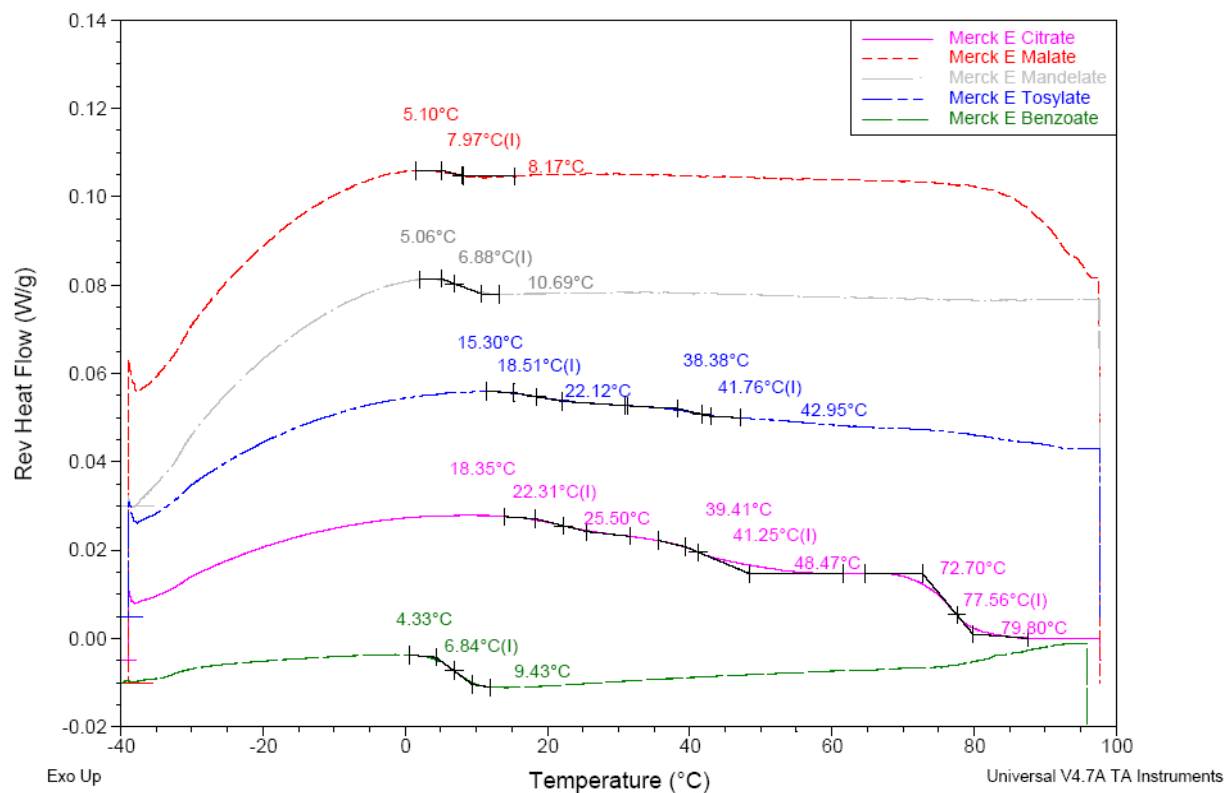


Figure B7. MK-E citrate (pink), malate (red), mandelate (silver), tosylate (blue), and benzoate (green) mDSC overlay with cycle 1 glass transition temperature indicated.

Appendix C: Dynamic Vapor Sorption (DVS)

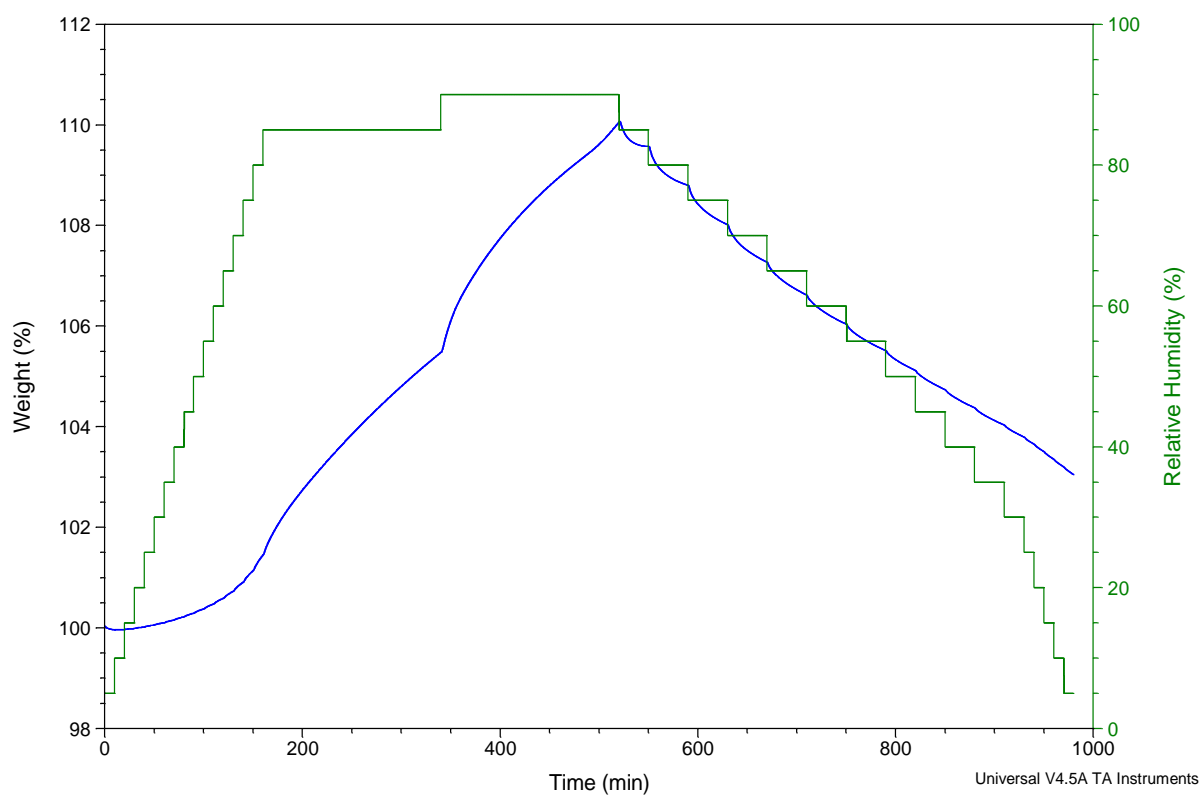


Figure C1. Lidocaine salicylate batch 3 DVS weight % and measured relative humidity vs. time plotted.

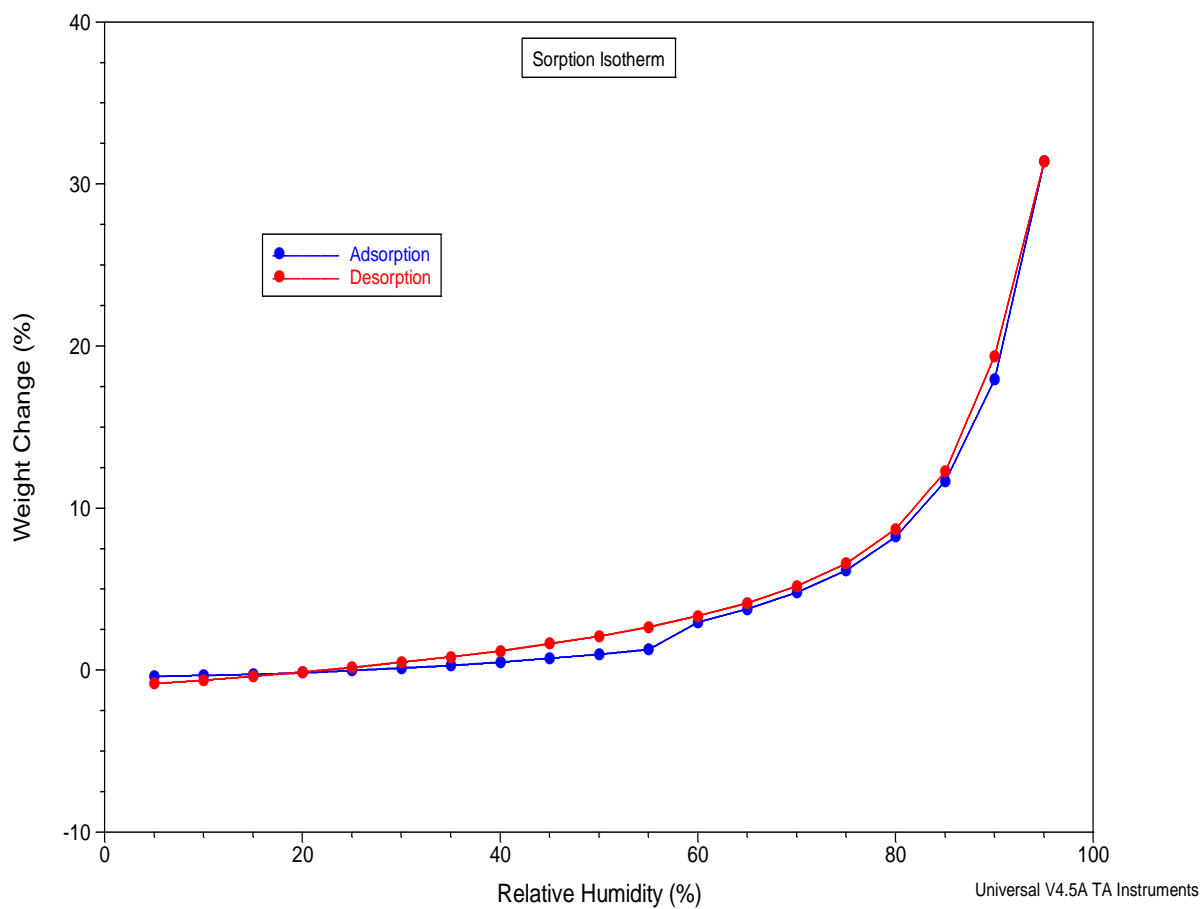


Figure C2. Lidocaine benzoate DVS relative humidity vs. weight change % plot.

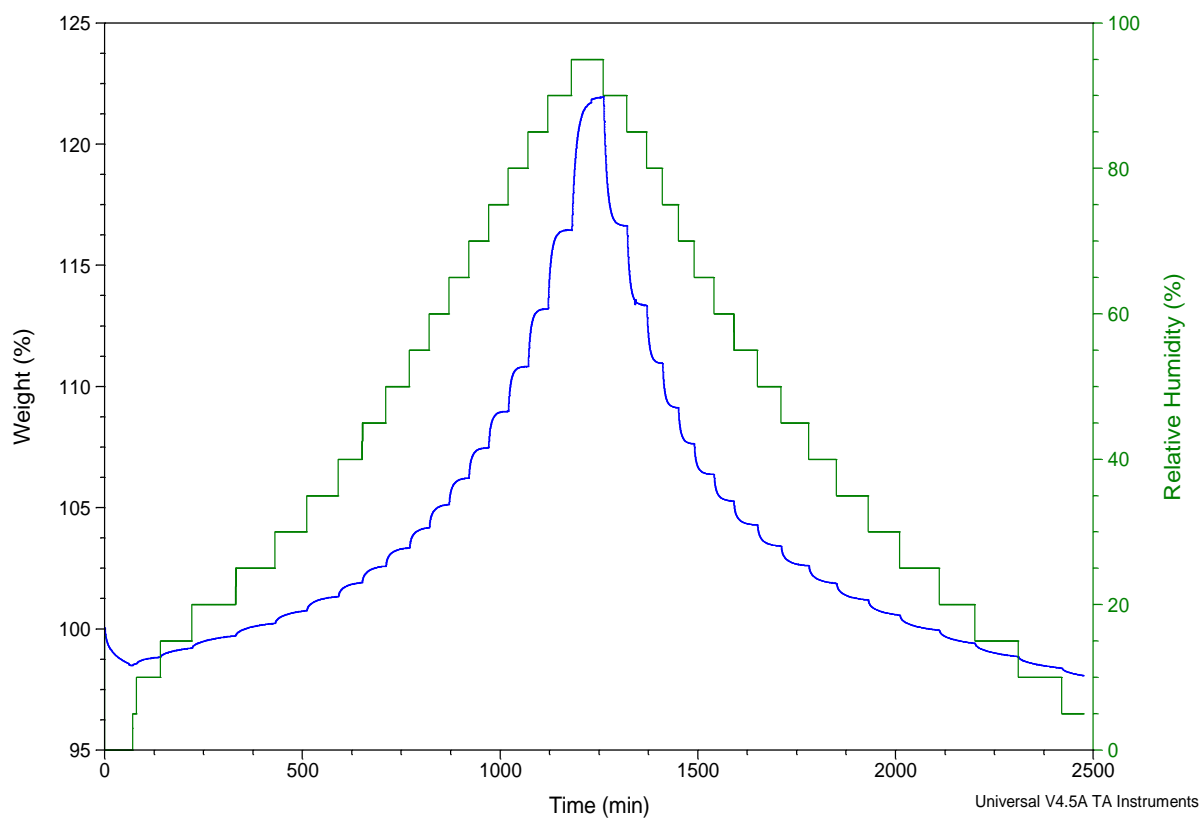


Figure C3. Propanteline tosylate DVS weight % and measured relative humidity vs. time plotted.

Appendix D: Nuclear Magnetic Resonance (NMR)

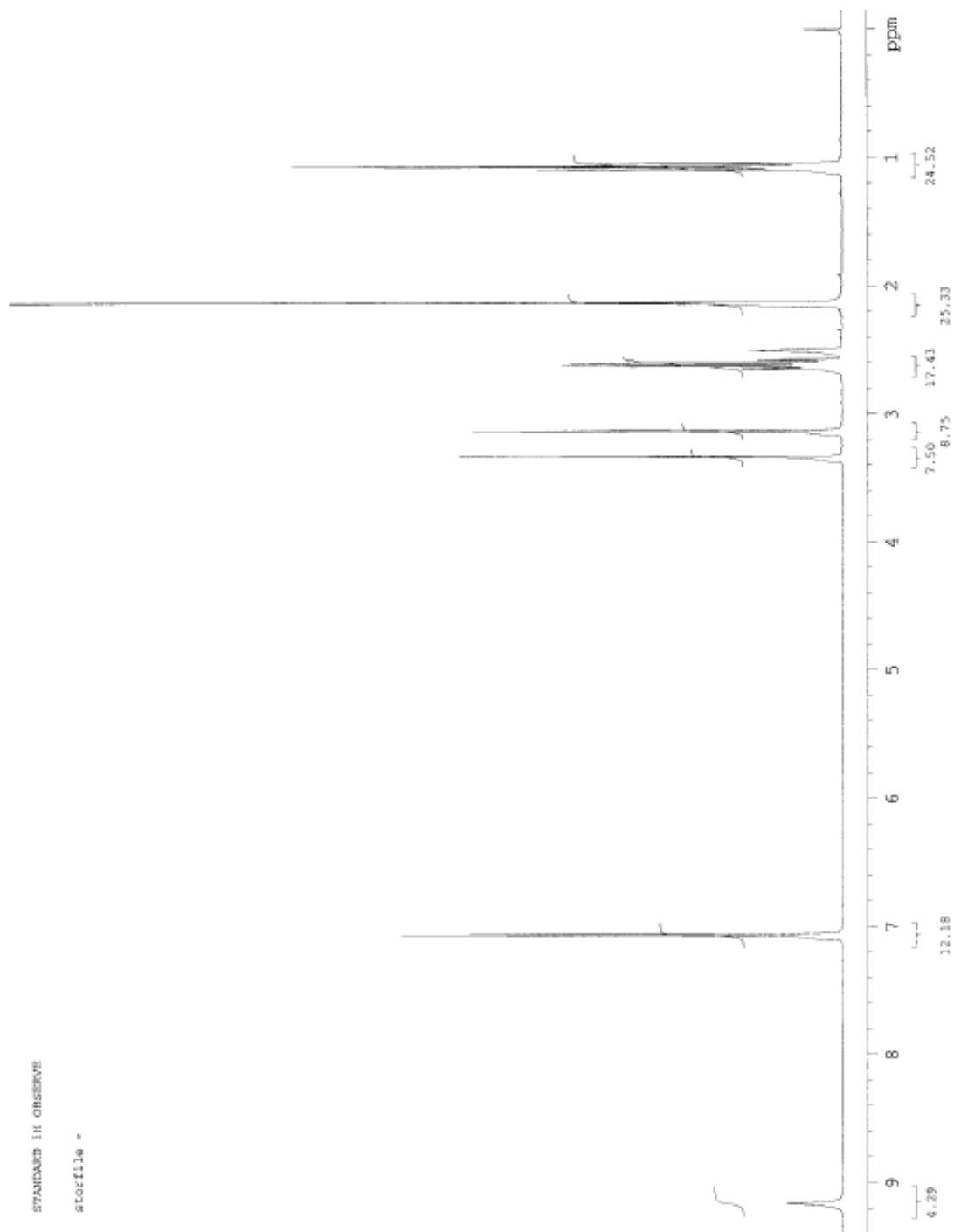


Figure D1. Lidocaine Standard NMR

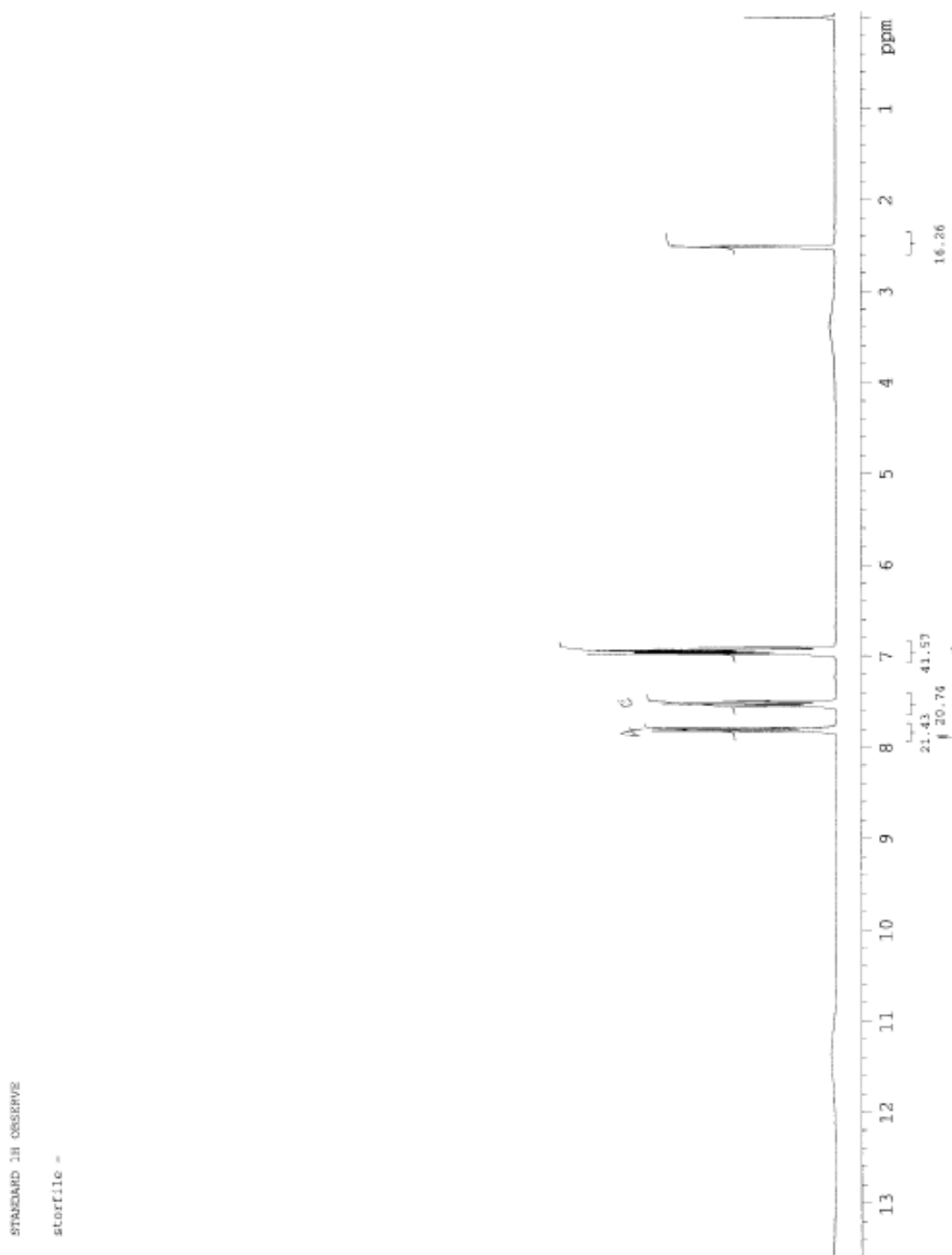


Figure D2. Salicylic acid standard NMR

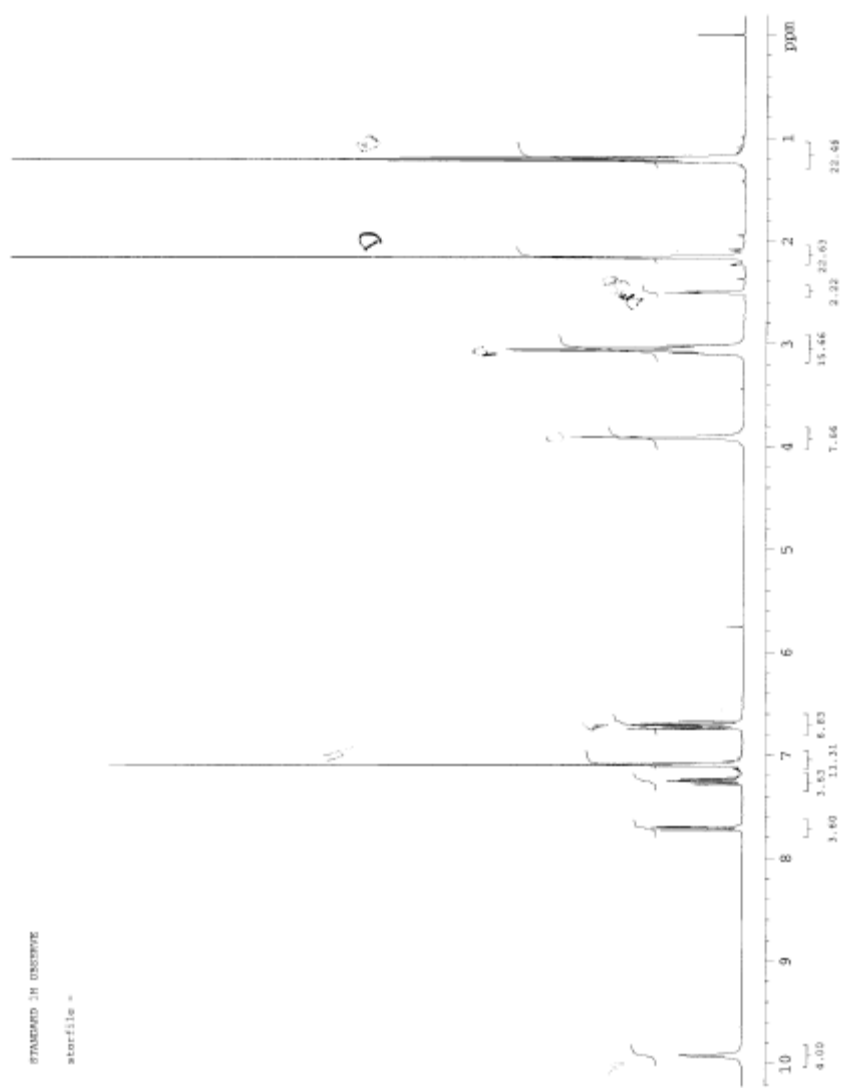


Figure D3. Lidocaine salicylate batch 3 NMR

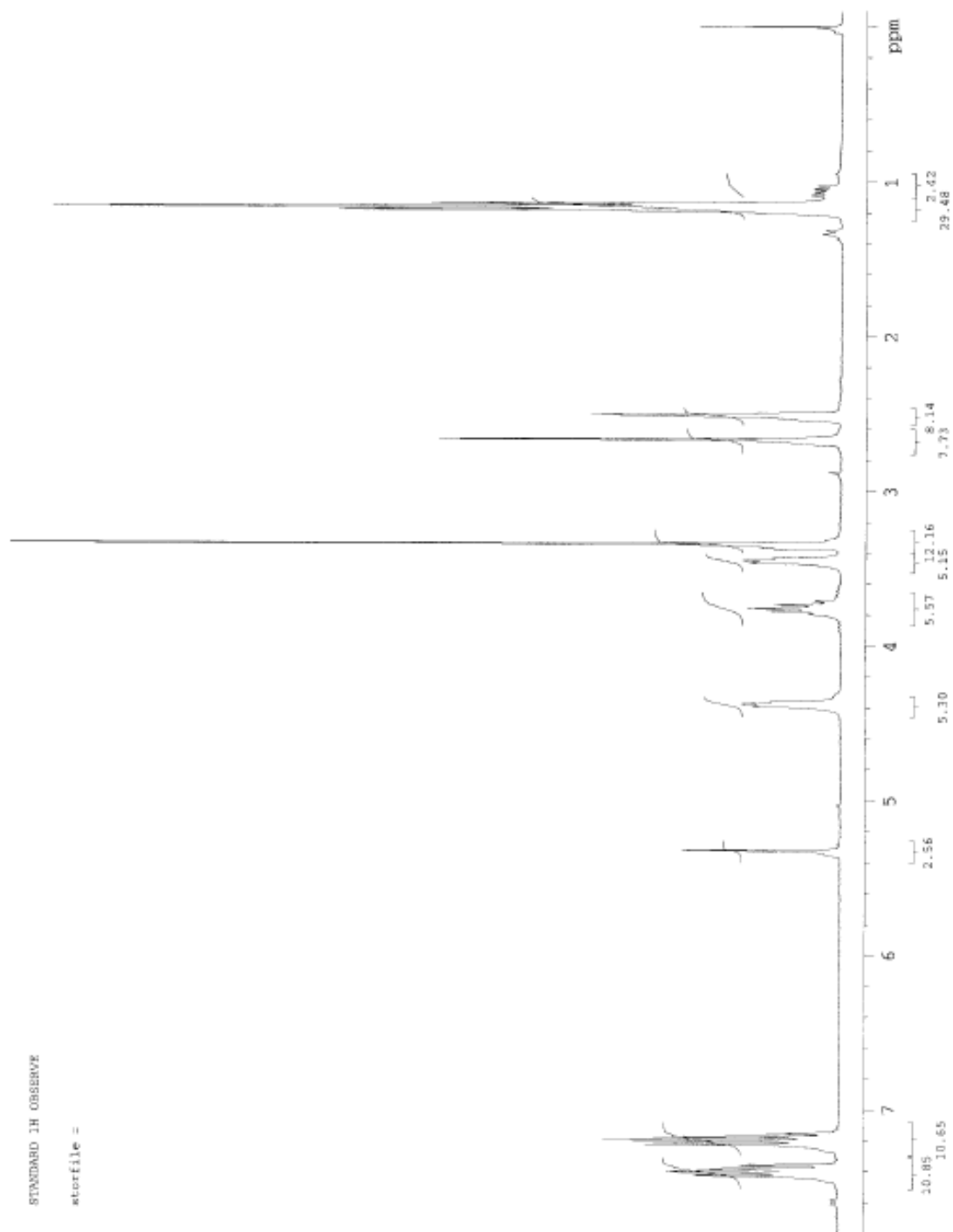


Figure D4. Propantheline Bromide standard NMR

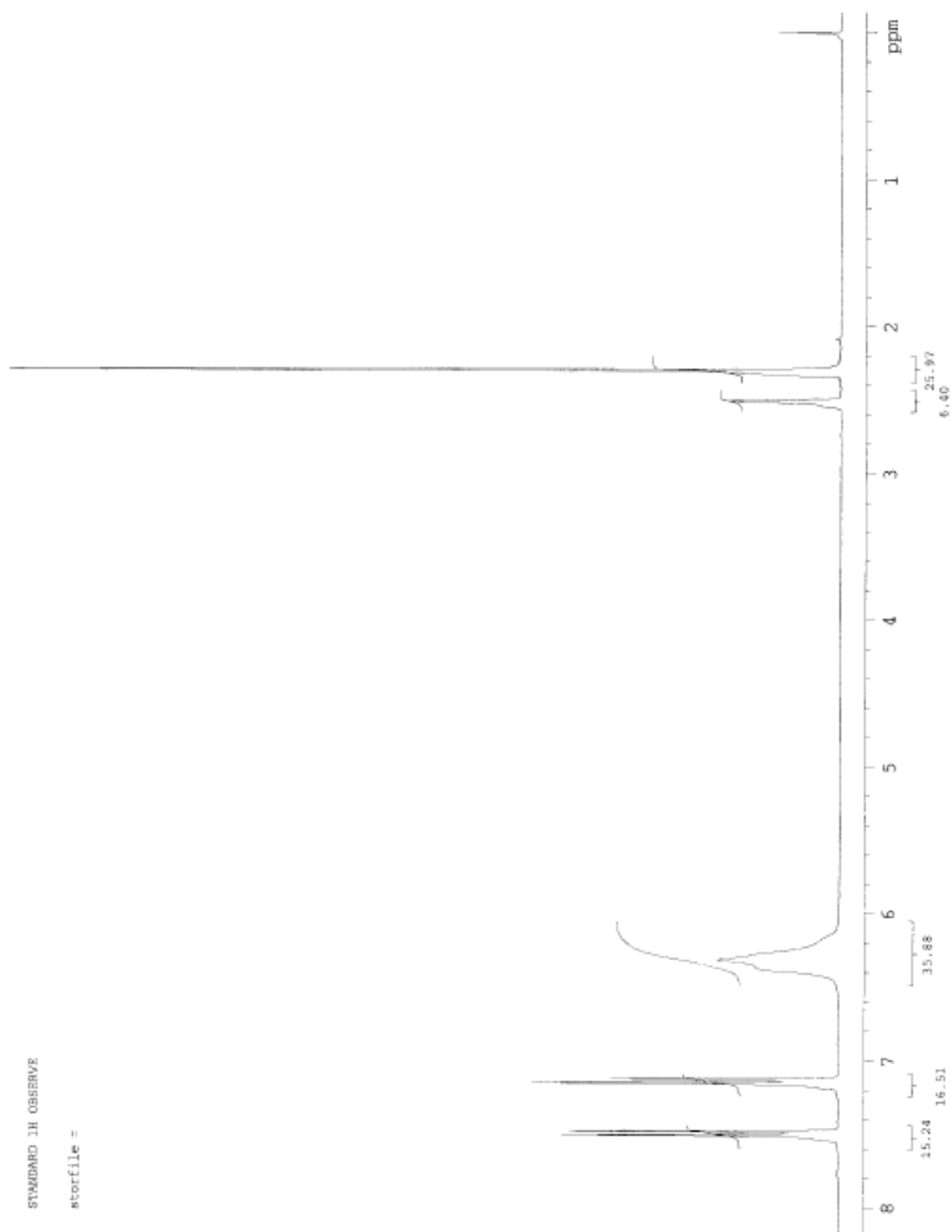


Figure D5. *p*-Toluenesulfonic Acid standard NMR

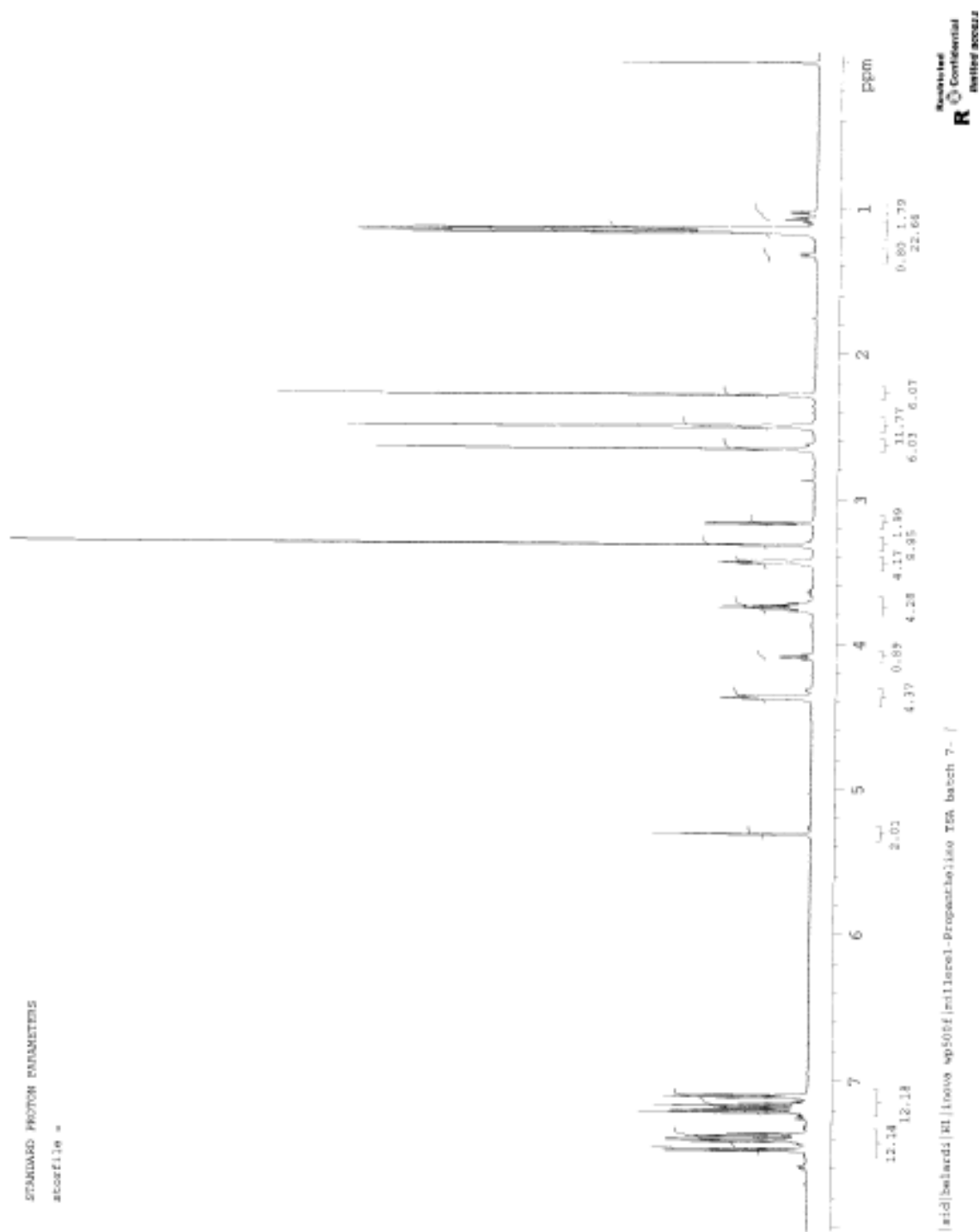


Figure D6. Propantheline tosylate NMR

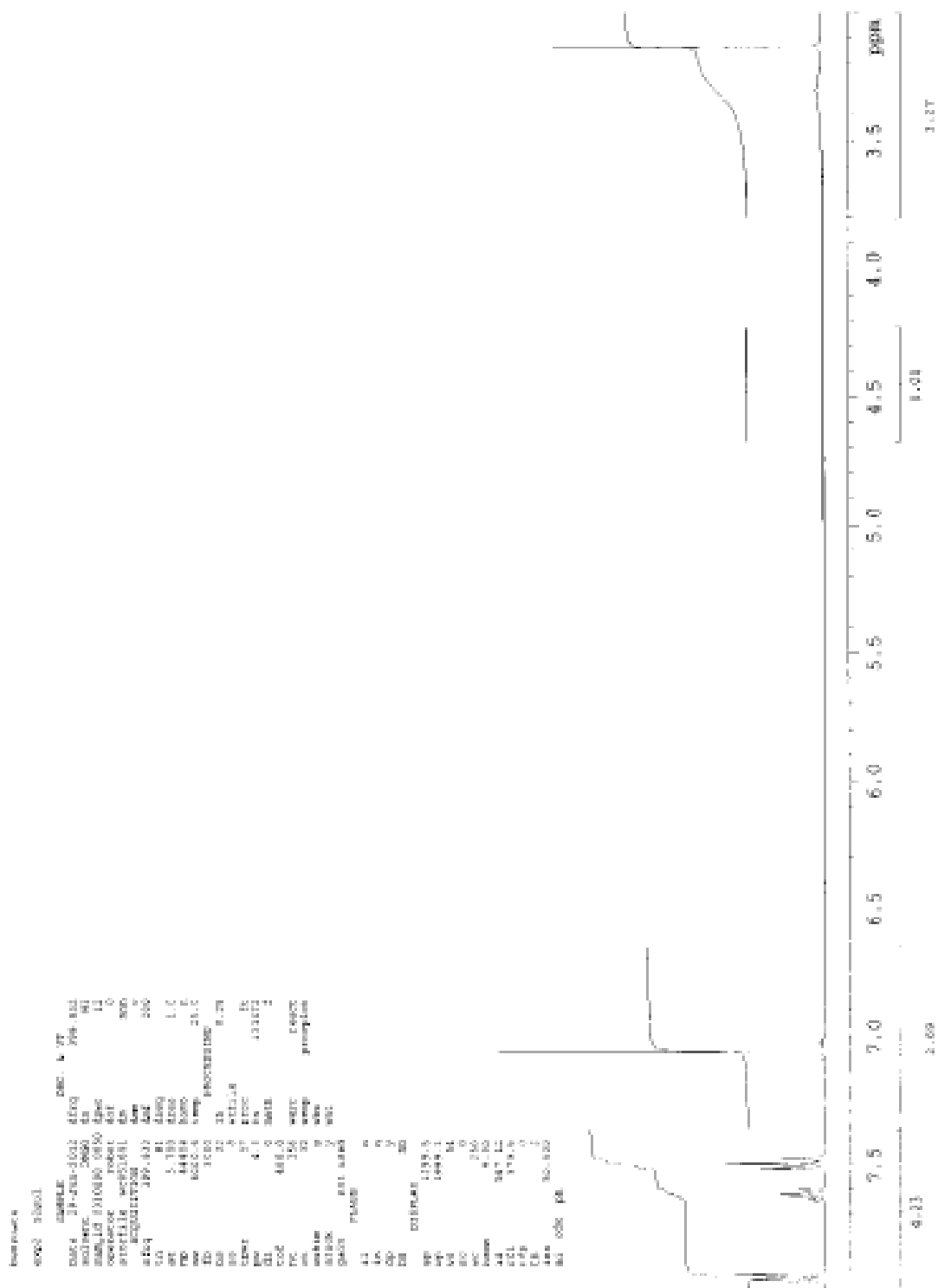


Figure D8. Lidocaine Benzoate NMR ranging from 3.5-7.5 ppm

Figure D10. Lidocaine Mandelate NMR

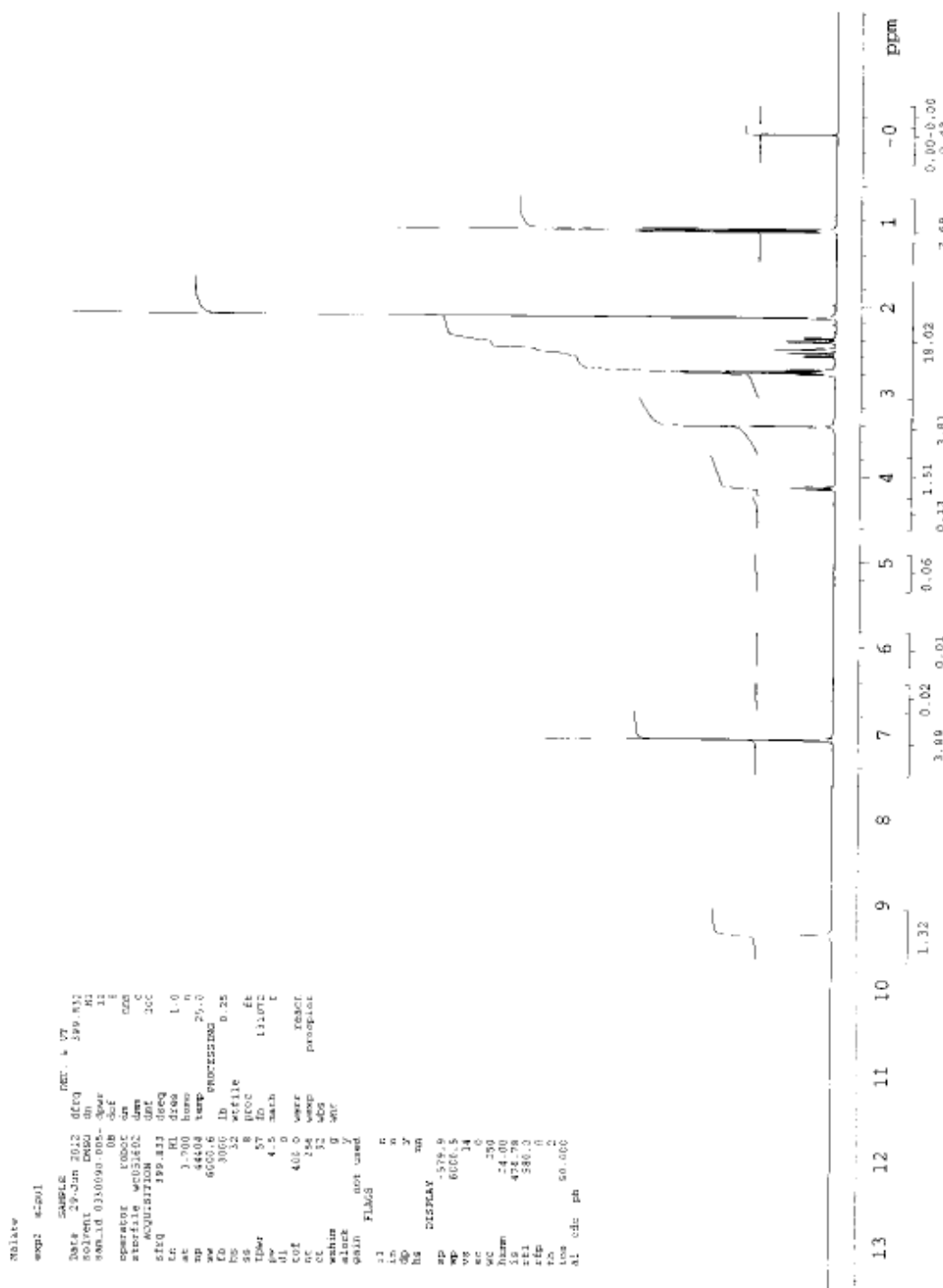


Figure D11. Lidocaine malate NMR

Appendix E: Viscosity

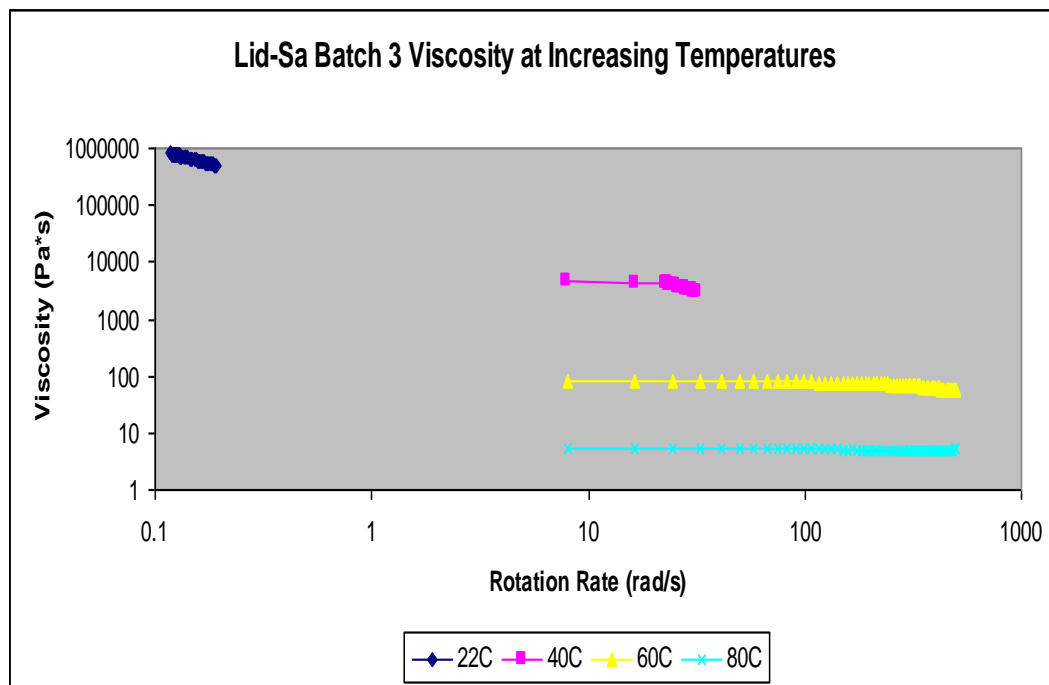


Figure E1. Lidocaine salicylate Batch 3 Viscosity vs. Temperature

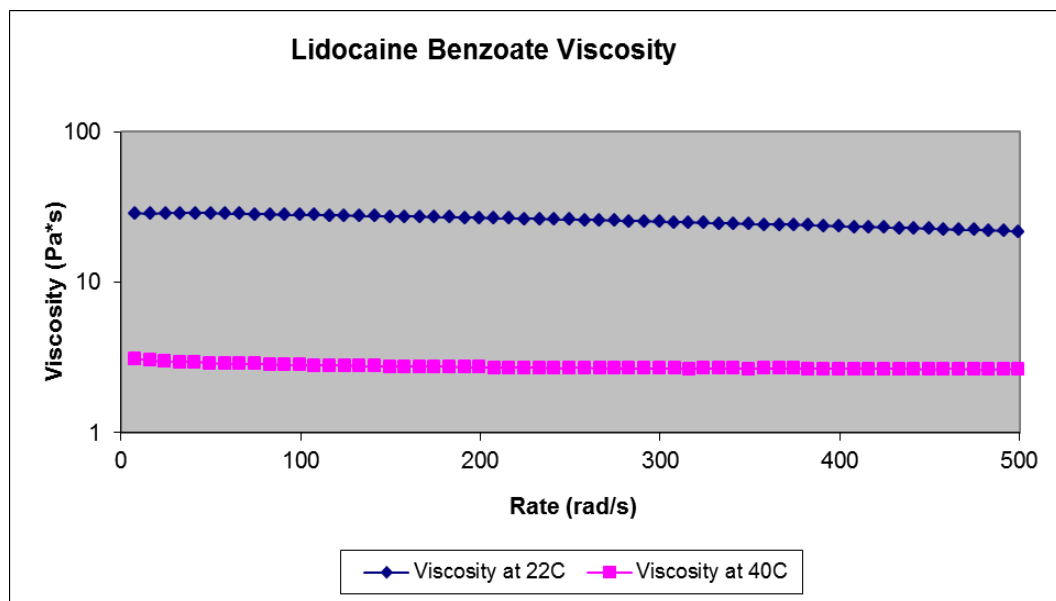


Figure E2. Lidocaine benzoate Viscosity vs. Temperature

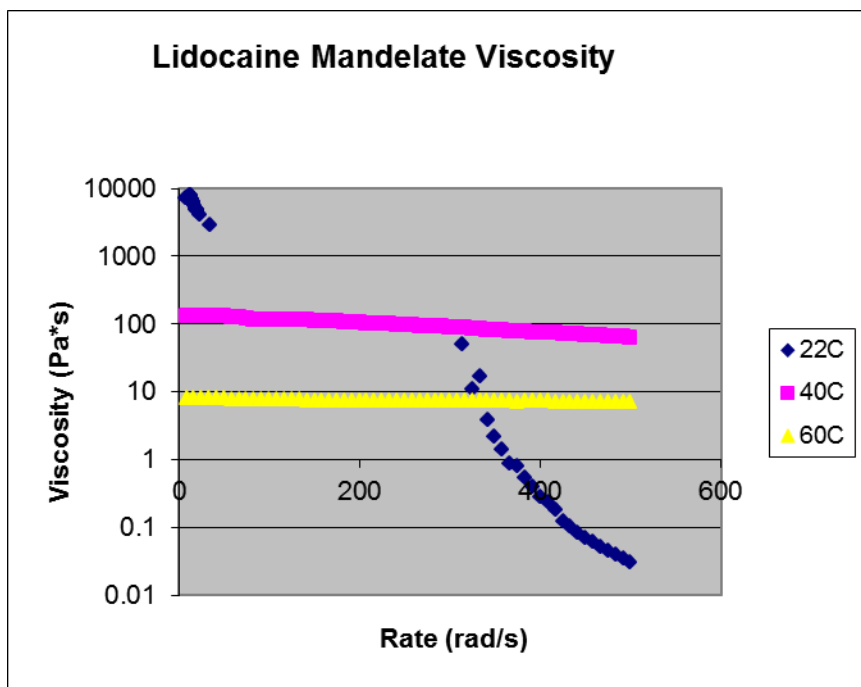


Figure E4. Lidocaine Mandelate Viscosity vs. Temperature

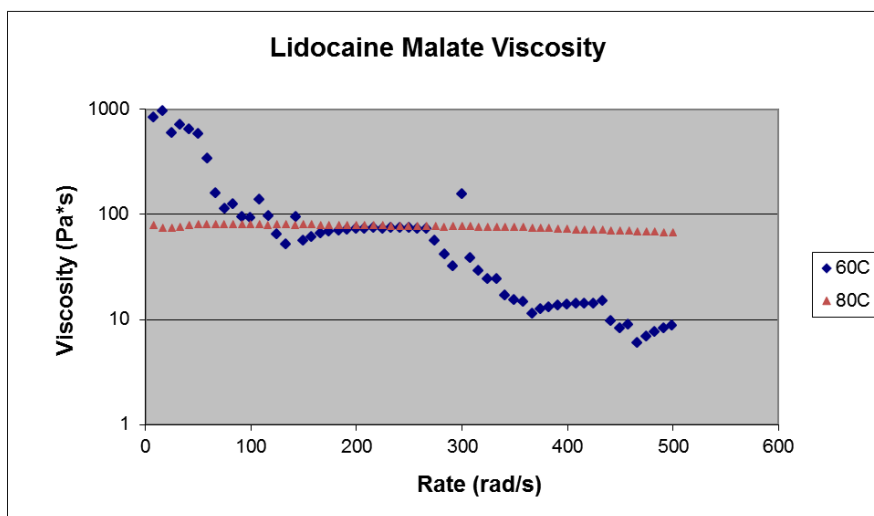


Figure E5. Lidocaine Malate Viscosity vs. Temperature

Appendix F: X-ray Diffraction (XRD)

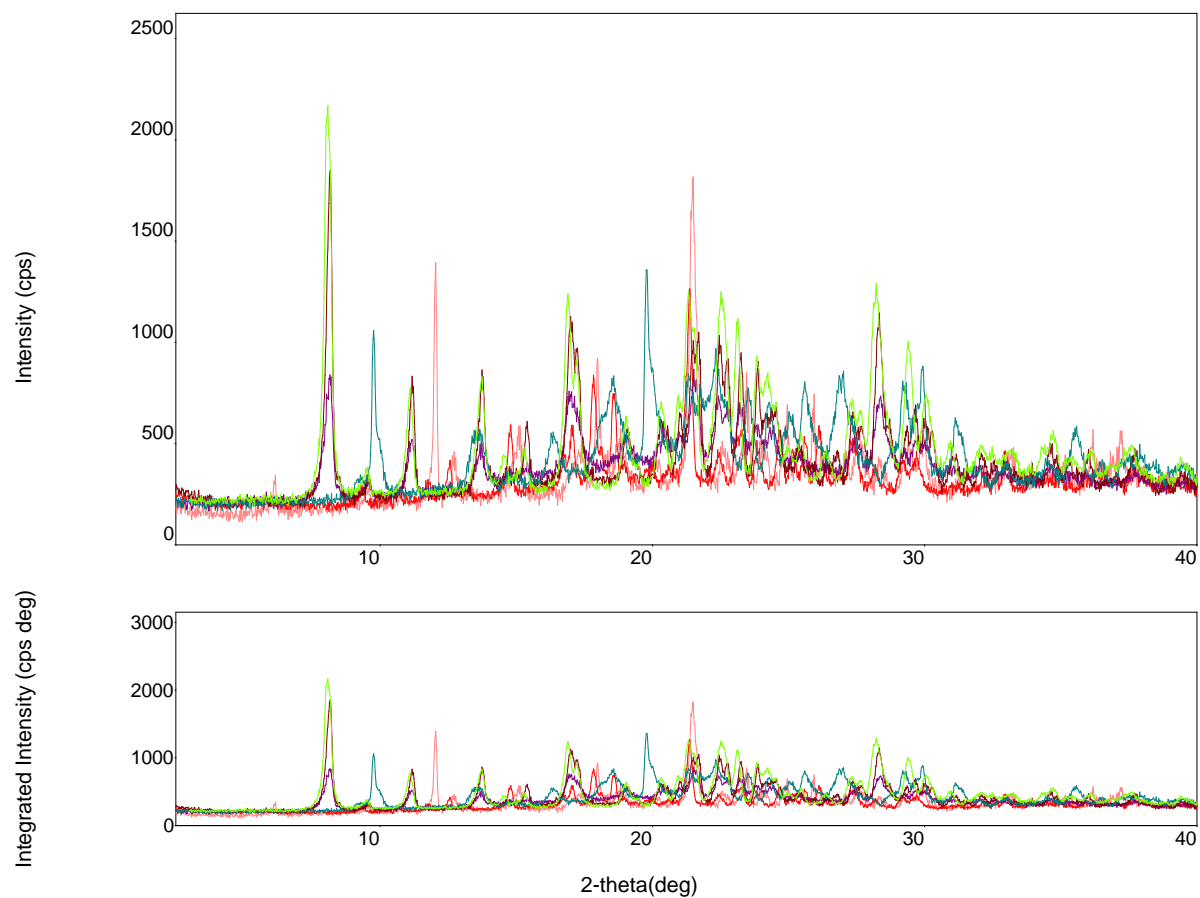


Figure F1. XRD overlay of MK-A acetate (pink), MK-A glutamate (red), MK-A MSA (purple), MK-A nicotinate (brown), MK-A salicylate (teal), and MK-A standard (green).

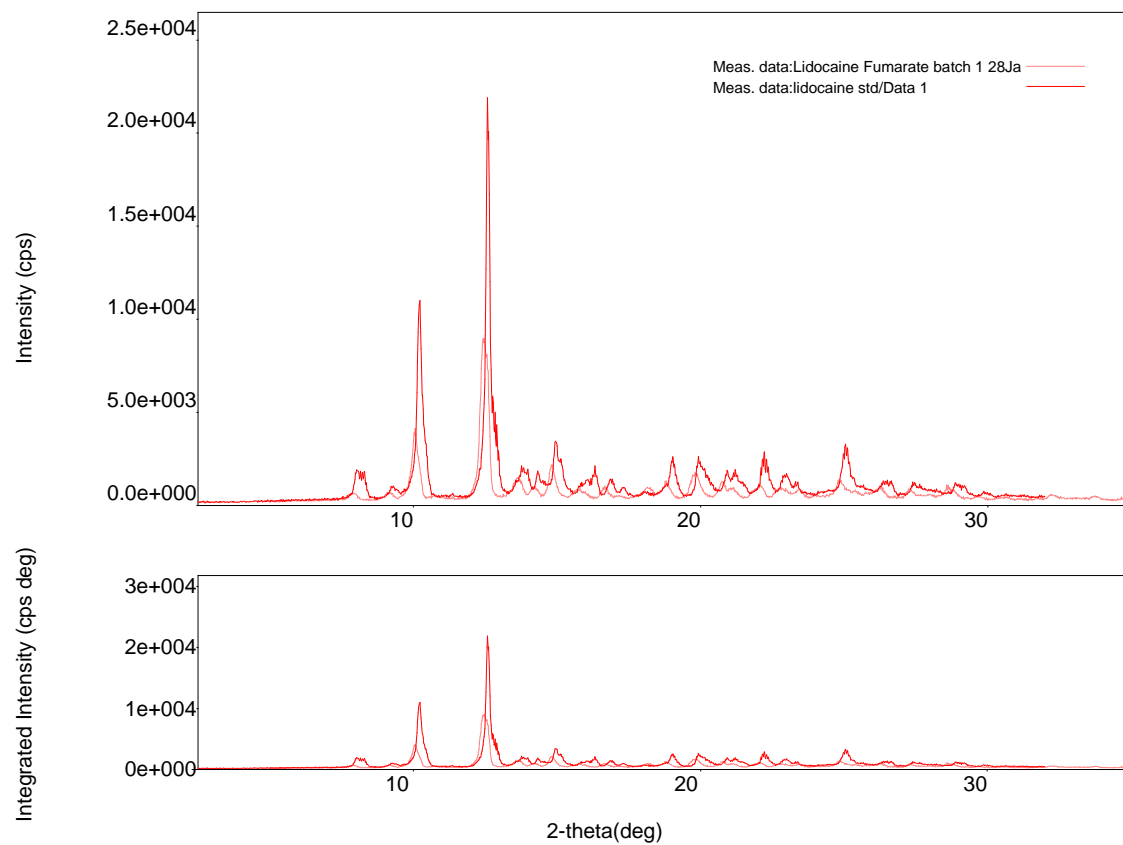


Figure F2. Lidocaine with Fumaric acid sample, lidocaine standard XRD pattern.

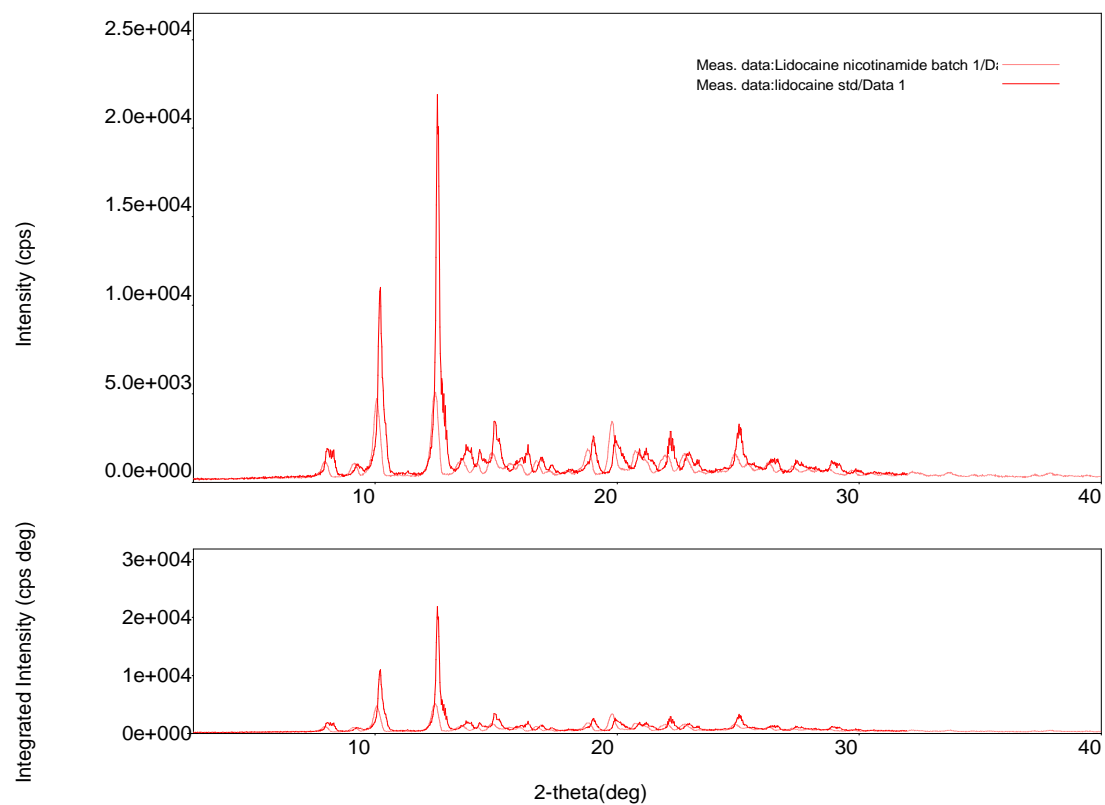


Figure F3. Lidocaine with nicotinic acid sample and lidocaine standard XRD pattern.

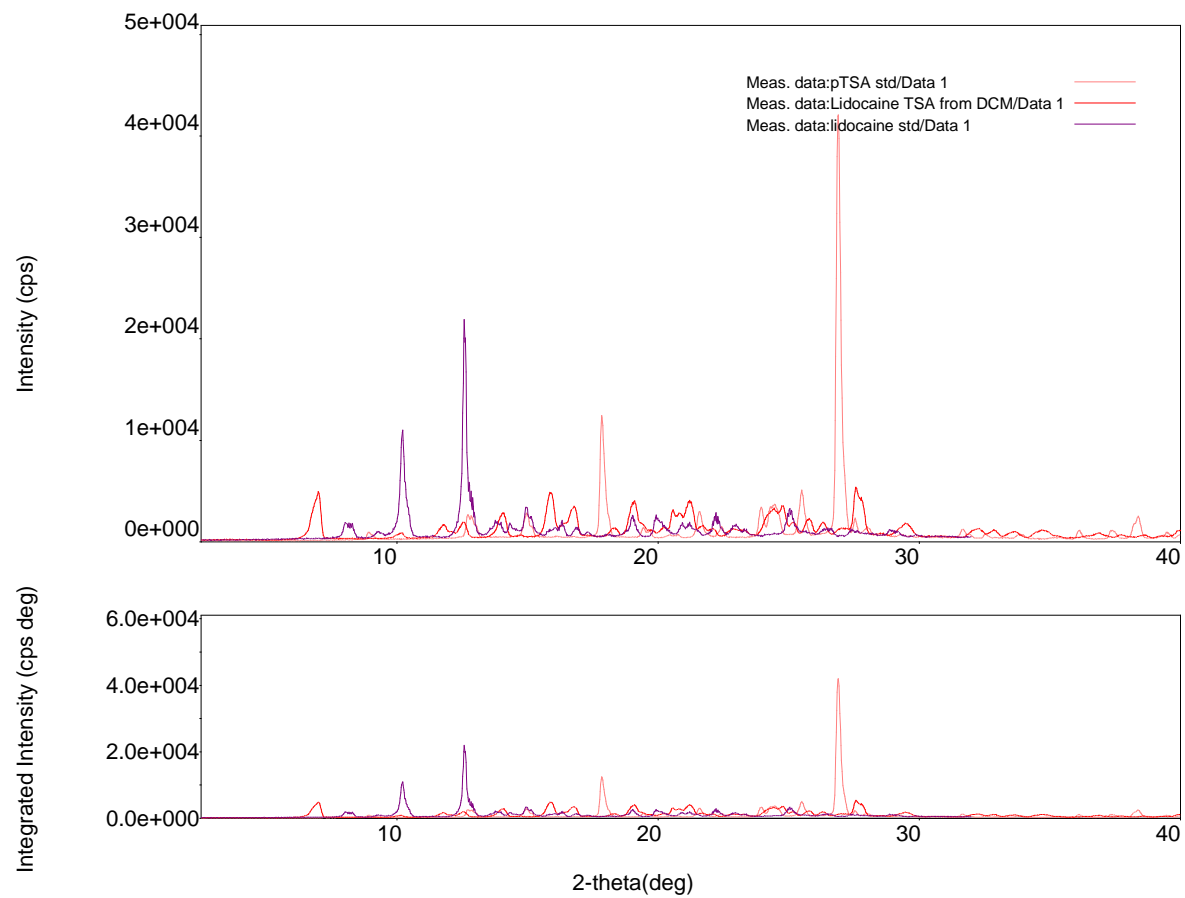


Figure F4. Lidocaine tosylate, lidocaine standard and tosylate standard XRD pattern.

Appendix G: Fourier Transform Infrared Spectroscopy (FTIR)

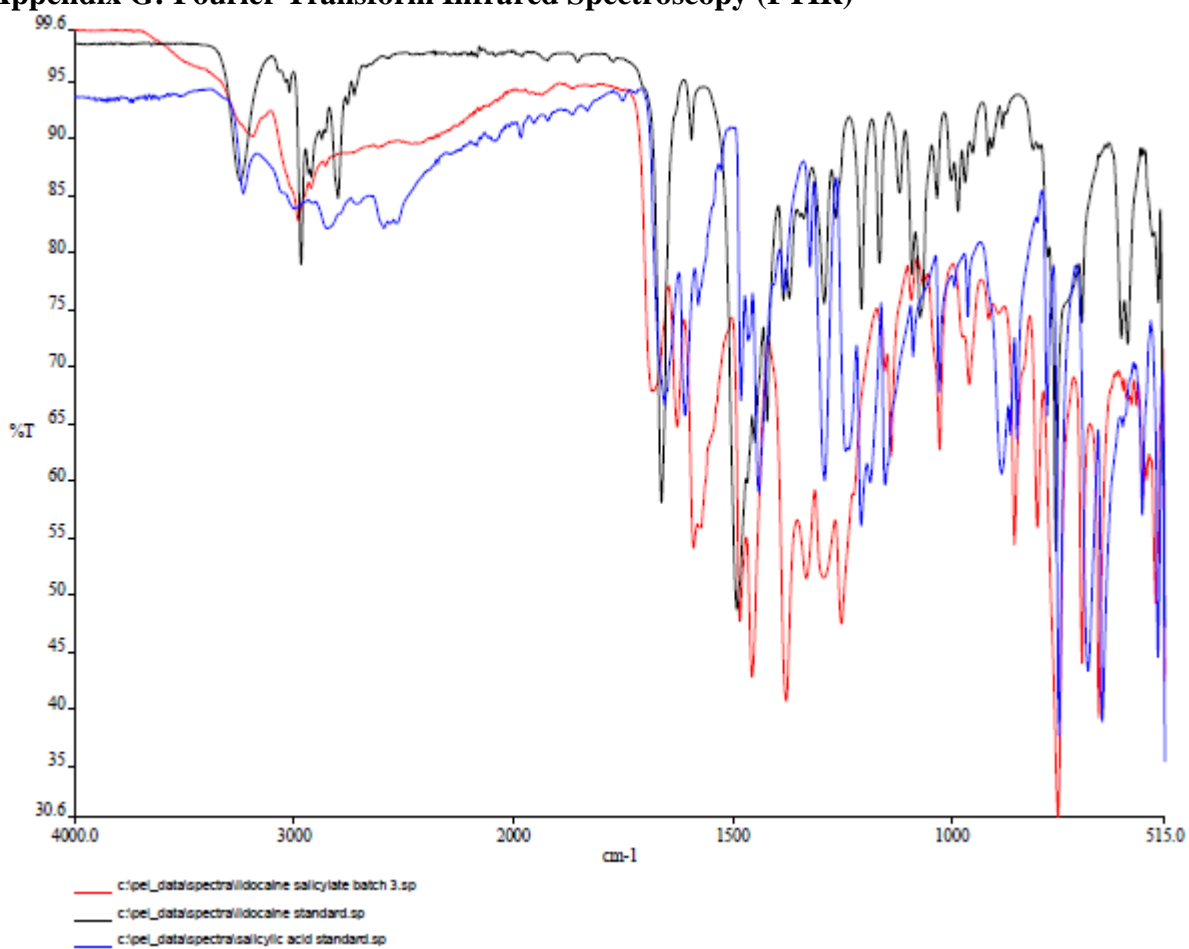


Figure G1 . Lidocaine salicylate (red), lidocaine standard (black), and salicylic acid standard (blue) IR spectra.

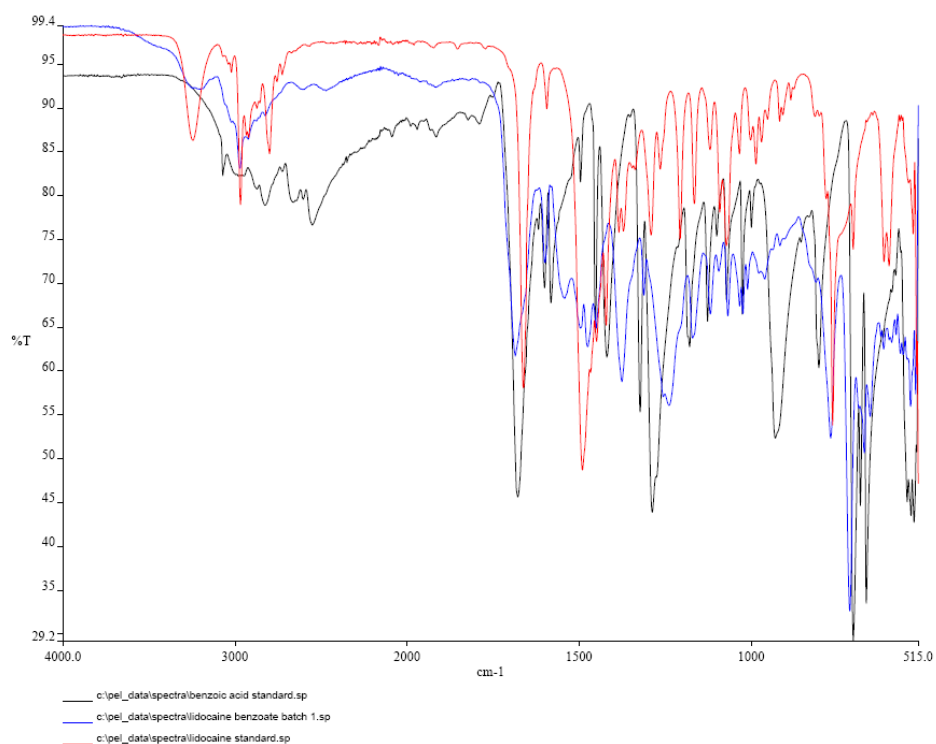


Figure G2. Lidocaine standard (red), benzoic acid standard (black), and Lidocaine benzoate (blue) IR spectra

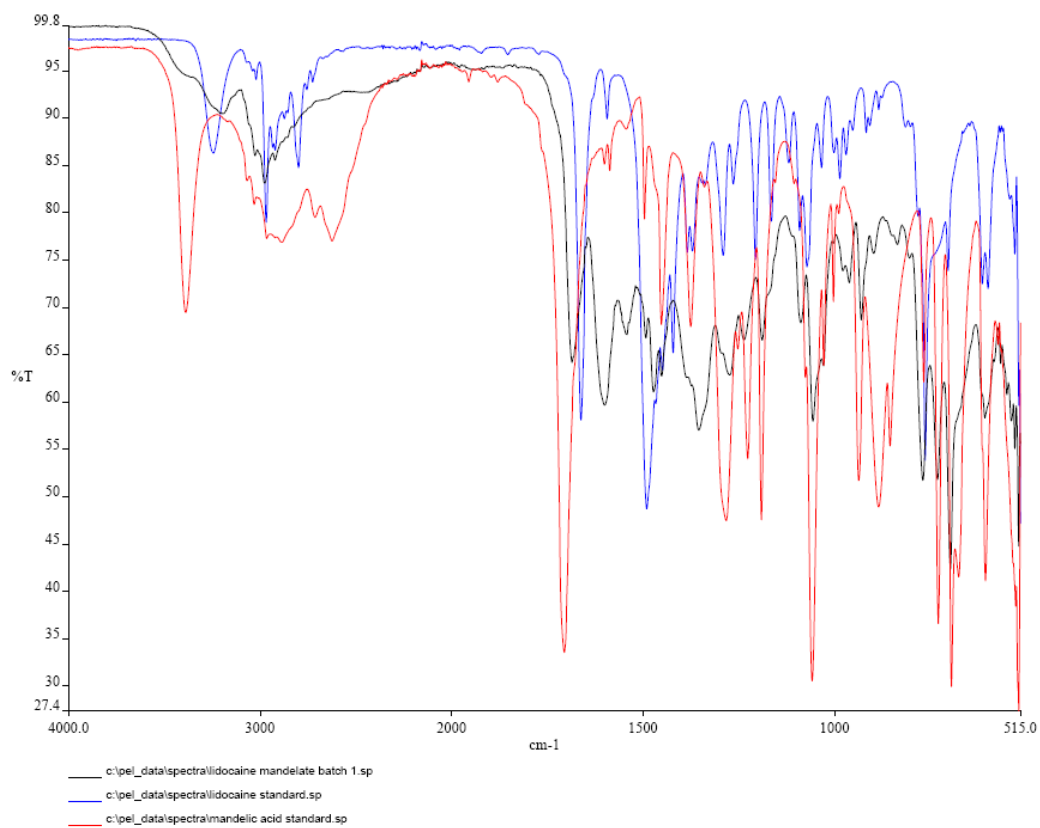


Figure G3. Lidocaine mandelate (black), Lidocaine standard (blue), and mandelic acid standard (red) IR spectra.

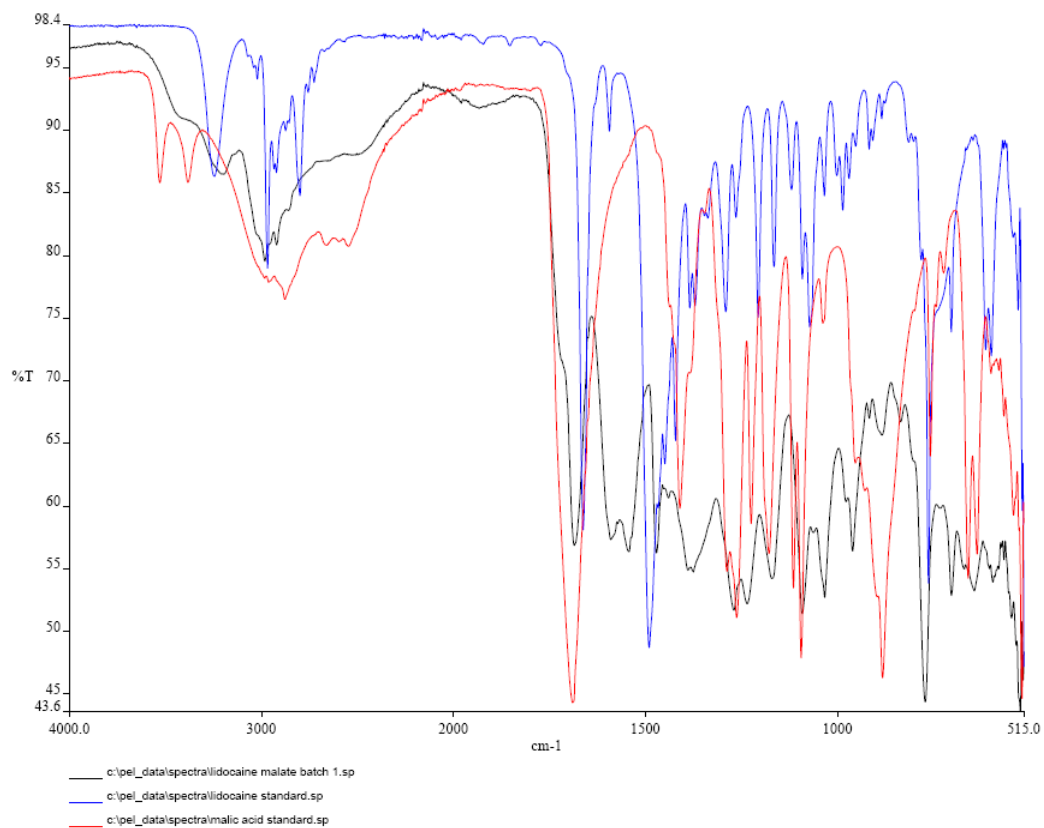


Figure G4. Lidocaine Malate (black), Lidocaine standard (blue) and malic acid standard (red) IR spectra.

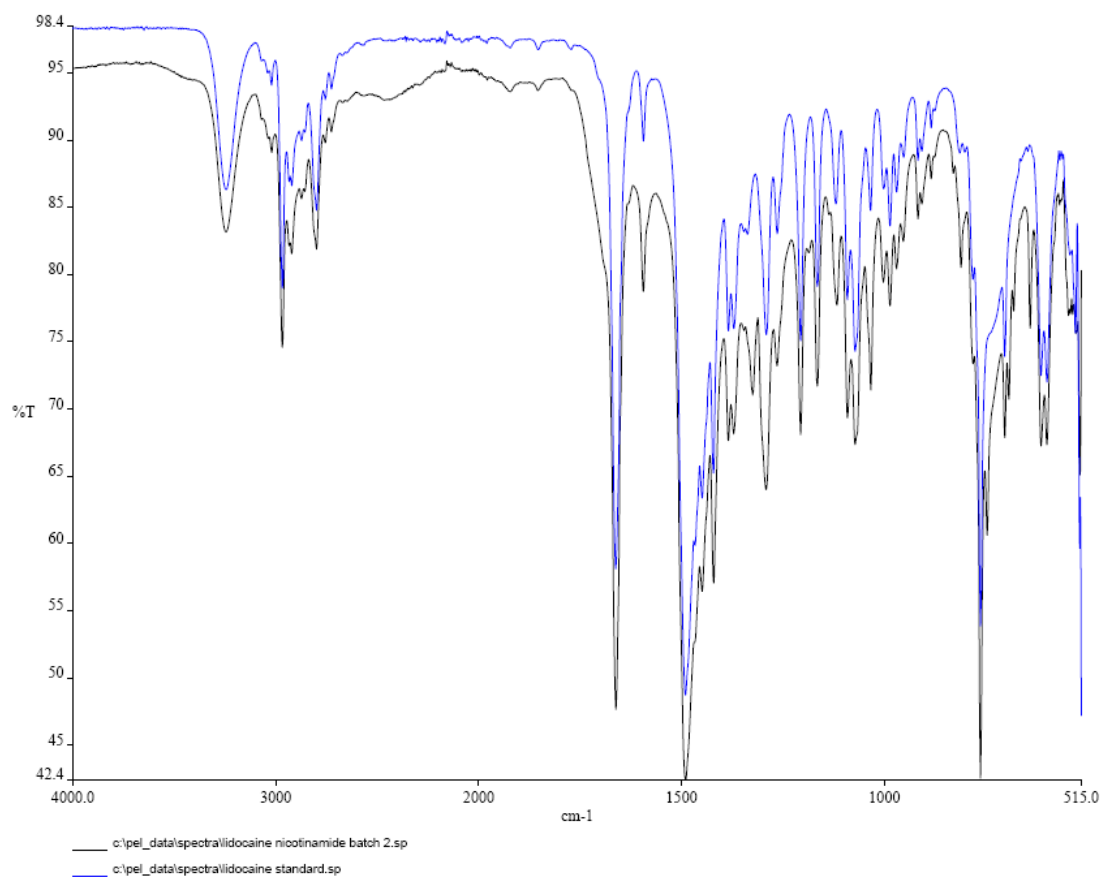
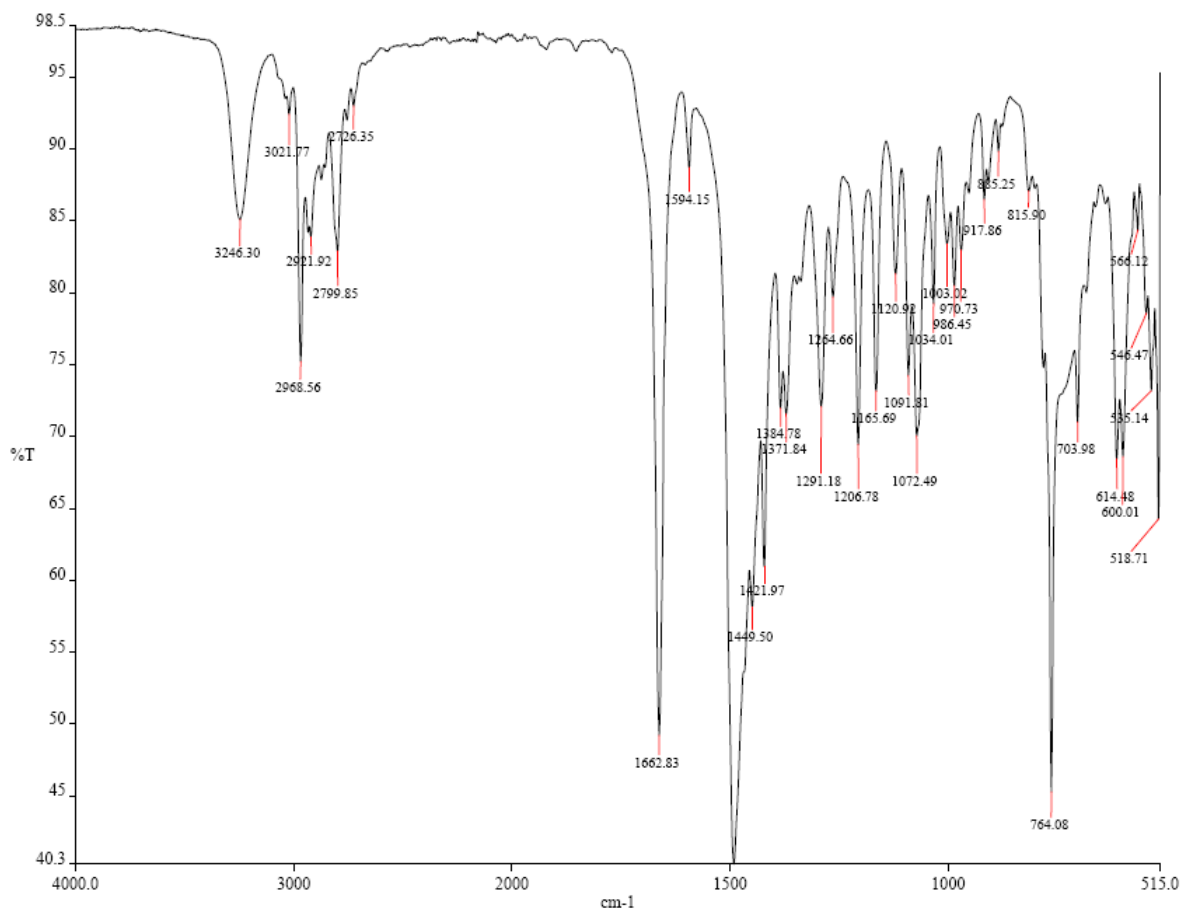


Figure G5. Lidocaine with nicotinic acid solids (black) and lidocaine standard (blue) IR spectra.



c:\pel_data\spectra\lidocaine fumarate batch 1.sp

Figure G6. Lidocaine with Fumaric acid sample IR spectra.